ORNL/TM-13170/V1

OAK RIDGE
NATIONAL
LABORATORY

LOCKHEED MARTIN

Characteristics of Spent Fuel from Plutonium Disposition Reactors

Vol. 1: The Combustion Engineering System 80+ Pressurized-Water-Reactor Design

B. D. Murphy

MANAGED AND OPERATED BY
LOCKHEED MARTIN ENERGY RESEARCH CORPORATION
FOR THE UNITED STATES
DEPARTMENT OF ENERGY

ORNL-27 (3-96)

ORNL/TM-13170/V1

Computational Physics and Engineering Division

CHARACTERISTICS OF SPENT FUEL FROM PLUTONIUM DISPOSITION REACTORS VOL. 1: THE COMBUSTION ENGINEERING SYSTEM 80+ PRESSURIZED-WATER-REACTOR DESIGN

B. D. Murphy

Date Published: June 1996

Prepared by the
Oak Ridge National Laboratory
Oak Ridge, Tennessee 37831-6370
Managed by
LOCKHEED MARTIN ENERGY RESEARCH CORP.
for the
U.S. DEPARTMENT OF ENERGY
under contract DE-AC05-96OR22464

CONTENTS

Page

LIST OF FIGURES

LIST OF TABLES

ACKNOWLEDGMENTS

Completion of this work was greatly facilitated by the efforts of R. T. Primm, III, with whom the author had many helpful technical discussions. The author would also like to acknowledge discussions on many details of the SCALE system with O. W. Hermann.

ABSTRACT

This report discusses a simulation study of the burnup of mixed-oxide fuel in a Combustion Engineering System 80+ Pressurized-Water Reactor. The mixed oxide was composed of uranium and plutonium oxides where the plutonium was of weapons-grade composition. The study was part of the Fissile Materials Disposition Program that considered the possibility of fueling commercial reactors with weapons plutonium. The isotopic composition of the spent fuel is estimated at various times following discharge. Actinides and all significant fission products are considered. The activities, decay-heat values, and gamma-ray fluxes associated with the spent fuel are also discussed. It is clear from the analysis that following discharge the plutonium is no longer of weapons-grade composition. The characteristics of the mixed-oxide fuel at various times following discharge indicate its behavior under long-term storage. As a counterpoint to the mixed-oxide fuel case, the situation with a similar reactor fueled with uranium oxide alone is analyzed. The comparisons serve to emphasize the significance of the plutonium as part of the fuel. For the mixed-oxide case, the burnup was 42,200 MWd/MTHM; in the pure-uranium case, it was 47,800 MWd/MTHM.

1. INTRODUCTION

As part of the Fissile Materials Disposition Program (FMDP), studies were conducted on the operation of reactors with mixed-oxide (MOX) fuel that contained oxides of weapons-grade plutonium, together with uranium oxide. These studies were conducted for a variety of existing reactor designs. CANDU, CANFLEX, standard BWR, Westinghouse, and Combustion Engineering System 80+ designs were considered. The characteristics of spent fuel in such instances are important for decision-making purposes related to the disposition of fissile material. Various reports were compiled detailing such characteristics and comparing spent fuel originating from admixtures of weapons-grade plutonium with regular uranium fuel.

This report discusses spent MOX fuel from a CE System 80+ reactor.[1] These studies were necessary for verification of the ref. 1 studies and to provide additional spent fuel characteristics that were not specified in ref. 1. These data were input to the Reactor Alternatives Summary Report currently in draft form and due to be issued by the Department of Energy in the spring of 1996. We will use the term MOX to refer to mixed oxides of uranium and plutonium with the further understanding that for the plutonium (which represented 6.7 wt % of the heavy metal) the isotopic content is of weapons-grade composition. For comparison purposes, this report also considers the spent fuel characteristics of a System 80+ reactor operating with conventional uranium-oxide fuel. Thus we will be discussing two cases: the uranium/plutonium MOX case and the uranium case. We will on occasion refer to the former as the plutonium case. The discussions below detail the characteristics of the spent fuel in a System 80+ assembly following burnup in the reactor core.

2. CHARACTERISTICS OF THE FRESH MOX FUEL ASSEMBLY

The fuel to be burned in the System 80+ is a MOX consisting of plutonium and uranium oxides, together with a small amount of erbia (Er_2O_3). The weapons-grade plutonium accounted for 6.7 wt % of the heavy metal in the core. The balance of the heavy metal consisted of uranium tails (0.2 wt % ^{235}U, with the remainder considered as ^{238}U). The core also contained Al_2O_3–B_4C in burnable poison rods (BPRs). The isotopic distribution of the plutonium was as follows (wt %): ^{238}Pu: 0.03; ^{239}Pu: 93.75; ^{240}Pu: 5.7; ^{241}Pu: 0.5; and ^{242}Pu: 0.02.

A System 80+ assembly is capable of containing 256 fuel rods in a 16 × 16 square array. An assembly with 16 rods on a side measures 202.5 mm, and the fuel-rod pitch is 12.9 mm. However, because of control rod holes, instrument holes, and BPRs, there is usually not a full complement of 256 fuel rods present. The assembly that was studied consists of 224 fuel rods. The detailed characteristics of these fuel rods are shown in Table 1.

The total density of plutonium atoms was equal to the total given in Table 3.1.7-4 of ref. 1. These densities were distributed among mass numbers 238, 239, 240, 241, and 242 according to the isotopic distribution noted previously (only ^{239}Pu and ^{240}Pu were quoted in Table 3.1.7-4 of ref. 1). The uranium number densities in Table 1 are determined from the assumption that the plutonium accounts for 6.7 wt % of the heavy metal. The erbium, in turn, is based on 1.6 wt % Er_2O_3 in the MOX pellets.

The nuclear data libraries in use contained only data on ^{166}Er and ^{167}Er. Thus although other isotopes of erbium were present, and since ^{167}Er was the only one that was of neutronic interest, ^{166}Er was substituted in place of all non-^{167}Er (a negligible amount of ^{167}Er was produced during irradiation). For the dose-rate estimates, since erbium was not available in the gamma data library, gadolinium was substituted. As this step involves only shielding calculations, and since gadolinium and erbium have similar atomic numbers, gadolinium is an acceptable substitute.

A variety of assemblies are present in the System 80+ core. The one studied is known as a 12-shim assembly. It contains five holes [four control-rod (CR) holes and one instrument-tube (IT) hole] plus 12 BPRs. As already mentioned, this assembly allows for 224 fuel rods. The System 80+ 12-shim assembly is depicted in Fig. 1. The CR holes and the IT hole each take up the space of four fuel rods (i.e., 20 fuel rods in all). Each BPR takes up the space of one fuel rod. Thus the total number of available fuel-rod spaces is reduced from 256 to 224. Data on fuel- rod and BPR sizes are contained in Table 1.

For BPR material (Al_2O_3–B_4C), the aluminum oxide was distributed in the rods with its normal density of 3.72 g/mL. The B_4C was distributed such that the ^{10}B loading was 0.0102 g/cm in each rod.

The assembly consisting of 224 fuel rods has a heavy-metal (HM) content of 0.419 metric tons (MT). The burnup criterion used was 42,200 MWd/MTHM. Thus the assembly was burned to 17681.8 MWd. In four cycles of 365 d each, this amount translates to an assembly power level of 12.11 MW (reactor power of 2.85 GWt). A 30-d downtime was allowed between cycles.

Table 1. Parameters for the MOX-fueled case

Fuel material radius	0.421 cm
Clad thickness	0.064 cm
Length of fuel pin	381 cm
Fuel material consisted of PuO_2, UO_2 and Er_2O_3	
Clad material: Zircaloy	
Fuel material densities (number/barn·cm)	
^{238}Pu	4.5976×10^{-7}
^{239}Pu	1.4307×10^{-3}
^{240}Pu	8.6626×10^{-5}
^{241}Pu	7.5672×10^{-6}
^{242}Pu	3.0144×10^{-7}
Uranium densities (number/barn·cm)	
^{235}U	4.2052×10^{-5}
^{238}U	2.0719×10^{-2}
Erbium densities	
^{166}Er	4.8430×10^{-4}
^{167}Er	1.4709×10^{-4}
BPR outside diameter	0.87 cm
Cladding thickness	0.064 cm

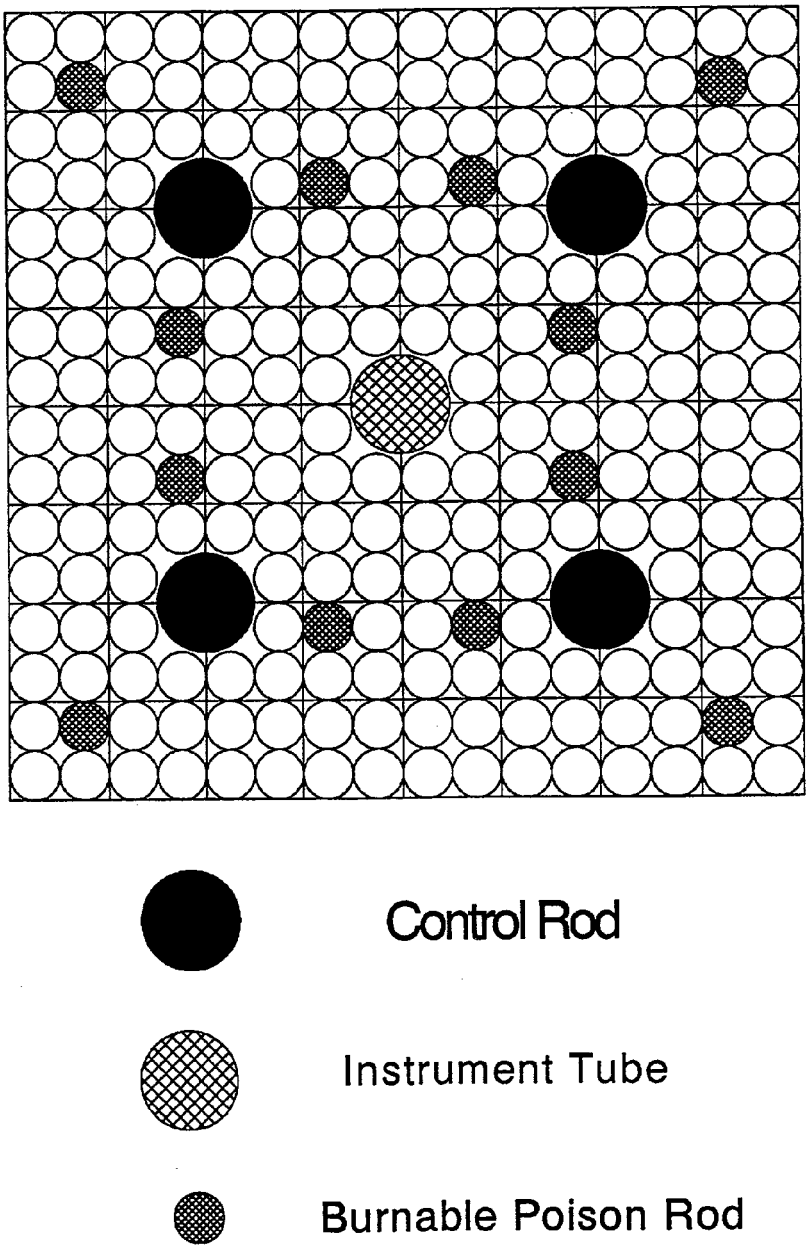

Fig. 1. Cross section of the Combustion Engineering System 80+ 12-shim fuel assembly.

3. CHARACTERISTICS OF THE FRESH URANIUM FUEL ASSEMBLY

As a counterpoint to the MOX (or plutonium) case, a conventional uranium-burning assembly was also studied. This assembly contained UO_2, with the ^{235}U enriched to 4.2 wt %. The purpose of studying a uranium-fueled assembly was to identify any increased hazards or risk of hazards of the MOX cycle relative to the existing low-enriched uranium (LEU) cycle. Note, however, that because of design requirements stipulated by Combustion Engineering, the two studies were less than ideal replicas of one another. Differences were observed in both the total burnup and the amount of heavy metal contained in the two assemblies. Ideally, one would like these two items to be consistent among the assemblies. In comparing results of the studies, one should, therefore, keep these differences in mind. We are concerned here with detecting differences significantly greater than burnup-related differences.

The assembly studied consisted of 236 fuel rods and contained five holes (four CR holes and one IT hole). Referring to Fig. 1, the CR and IT holes in total take up 20 spaces in the 16 × 16 array, thus leaving 236 of the 256 spaces for fuel rods. Of the 236 fuel rods, 12 were integral erbia burnable absorber rods. These burnable absorber rods consisted of 1.6 wt % erbia (Er_2O_3) uniformly mixed within the enriched fuel pellets. As opposed to the MOX case, the erbia was contained in only a subset of the fuel rods.

This erbia was modeled by specifying a thin erbia zone with the appropriate atom densities and at a representative radius in the assembly. Recall from Table 1 that in the plutonium (MOX) case, since erbium was mixed with all the fuel elements it was possible to specify it as part of the fuel mixture. These burnable absorber rods (containing both erbia and fuel) were located where the BPRs had been in the MOX case. (Note that the BPRs in the MOX case did not contain any fuel.) The characteristics of the fuel rods for the uranium case are given in Table 2.

The uranium densities are such that the number density of oxide molecules (UO_2 in this case) is equal to that in the plutonium-burning case (PuO_2, UO_2, and Er_2O_3). As in the plutonium (MOX) case, in making dose-rate estimates, gadolinium was used in place of erbium. Again, since only shielding calculations are involved, gadolinium is an acceptable substitute.

The total amount of heavy metal in the uranium-fueled assembly was 0.424 MT. The burnup was 47,800 MWd/MTHM. Thus the assembly was burned to 20267.2 MWd. In three cycles of 18 months each, this amounted to an assembly power level of 12.34 MW (reactor power of 2.62 GWt). A 30-d downtime occurred between cycles.

Table 2. Parameters for the uranium-fueled case

Fuel material radius	0.421 cm
Clad thickness	0.064 cm
Length of fuel pin	381 cm
Clad material: Zircaloy	
Uranium densities (number/barn·cm)	
^{234}U	8.5930×10^{-6}
^{235}U	9.6140×10^{-4}
^{236}U	4.4037×10^{-6}
^{238}U	2.1628×10^{-2}

4. SPENT FUEL CHARACTERISTICS AND COMPARISONS

This study seeks to find major differences between the characteristics of the spent fuel from a System 80+ burning MOX with weapons-grade plutonium and a System 80+ burning conventional uranium fuel. Furthermore, one wishes to determine if the plutonium discharged in the MOX case is of non-weapons grade. The characteristics of the spent fuel are of interest in assessing the hazards of spent fuel from the point of view of handling, transportation, and storage. Therefore, one examines such things as spent fuel isotopic concentrations, radiological activity, decay heat, and gamma and neutron doses under various conditions.

For most of the effects considered, the differences between the plutonium (MOX) and uranium cases are small. The differences that are of interest are those resulting from the replacement of some of the uranium with weapons-grade plutonium. Differences in burnup result in an obvious impact: in the uranium case, the burnup is 47.8 GWd/MTHM, and in the plutonium case, it is 42.2 GWd/MTHM. We are interested in determining if the differences following discharge are significantly greater than the perturbations introduced by different burn times.

4.1 COMPUTATIONAL METHODS

The results to be discussed were obtained by exercising the SAS2H, ORIGEN-S, and SAS1 codes. The SAS2H "code" is actually a driver program that invokes a sequence of codes in the SCALE[2] system. It models the burnup of a fuel assembly by determining assembly-averaged neutron spectra based on the fuel and structural composition of the assembly and the assembly power level. It then determines depletion, ingrowth, and decay of nuclear material, and it does so for each reactor cycle. The ORIGEN-S[3] code is employed to follow the inventory of nuclear material in the assembly after discharge from the reactor (ORIGEN-S is one of the codes employed in the SAS2H sequence). In the analyses following discharge, ORIGEN-S provides estimates of activities, decay heat, and hazards associated with the nuclear material. Using source terms calculated by ORIGEN-S, the SAS1[4] system was used to determine the dose rates from the assemblies (both shielded and unshielded) at various times following discharge. More specifically, the details of the calculations are explained in the following paragraph.

In order to calculate cross sections, SAS2H executes a two-step calculational process. The first step is the calculation of cell-weighted cross sections for a unit fuel-pin cell. In the second step, a larger unit cell representative of an assembly is considered. This larger cell is defined to represent the desired assembly design containing water holes, BPRs, cladding material, fuel rods containing absorbers, etc. It models the actual assembly by defining an equivalent with circular cylindrical symmetry. The fuel neutron flux spectrum obtained from this larger (cylindrical) unit cell is used to determine the appropriate nuclide cross sections for the burnup-dependent fuel compositions.

Two points are worth mentioning in connection with the two-step nature of these calculations: If the fuel itself were "smeared out" over the larger unit cell, resonance-self-shielding effects could not be considered. Hence the effective cross sections for the fuel rod are calculated in the first step, thereby accounting for resonance self-shielding. Second, the discrete-ordinates transport calculation assumes an azimuthal isotropy, which is achieved via the spatial averaging. Thus when XSDRNPM (see below) is referred to as being "one-dimensional," this description means that there is a variation in just one dimension (i.e., the radial direction).

SAS2H[5] is a component of the Shielding Analysis Sequence, known as SAS, that was developed for the SCALE-4 version. SAS2H calls ORIGEN-S so that the depletion and decay calculations can be carried out following library preparation. Before invoking ORIGEN-S, SAS2H calls three separate programs for the calculation of neutron cross sections:

BONAMI, a program to perform resonance shielding calculations through the application of the Bondarenko shielding factor method;

NITAWL-II, a program which applies the Nordheim Integral Technique to perform neutron cross-section processing in the resonance energy range; and

XSDRNPM, a discrete-ordinates transport code that is used in this sequence to produce cell-weighted cross sections.

BONAMI, NITAWL-II, and XSDRNPM are explained in ref. 2.

The ORNL code ORIGEN-S was employed to calculate the time evolution of the nuclide species in a typical assembly during burnup and following discharge. ORIGEN refers to the Oak Ridge Isotope Generation and Depletion code, and the S in ORIGEN-S indicates the version that is part of the SCALE system. ORIGEN-S calculates the time evolution of nuclide species at a typical point in an assembly, and it makes use of neutron-flux data, cross sections, and other neutronic data (e.g., fission-product yields, decay rates, branching fractions) that are representative of the assembly and its nuclide inventory as a function of time. Thus it determines the depletion of fissionable species, the ingrowth of actinides and fission products, and the subsequent decay and ingrowth of resulting nuclides over time. ORIGEN-S can also determine decay-heat source strengths, as well as radiation source spectra and strengths.

ORIGEN-S requires that the neutron energy spectrum, and hence the cross sections, be representative of a typical location in the assembly. Thus in order to exercise ORIGEN-S successfully it is necessary to prepare cross-section libraries that are representative of the assembly. The makeup of the assembly will vary with time, which in turn affects the neutron flux and thus the cross sections. Thus cross-section libraries must be adjusted over the course of the burnup history. In simulating burnup during reactor operation, all of these steps are taken care of in the SAS2H sequence. Following discharge, the time evolution of the nuclide species is calculated by using ORIGEN-S in its stand-alone version.

SAS1 is similar to SAS2H in that it replaces the actual assembly with a cylindrically symmetric equivalent. The radiation source strength of the assembly at various times following discharge (which had been calculated with ORIGEN-S) was then dispersed throughout this equivalent assembly. In this way SAS1 was used to calculate radiation dose rates in the vicinity of an assembly at various times following discharge.

The cross-section library used in the SAS2H calculations is known as the 44-group ENDF/B-V library. This 44-group library is specifically designed for the analysis of fresh and spent fuel and radioactive waste systems. For the shielding analysis performed with SAS1, the 27n-18g coupled library was used. This library consists of 27 neutron groups and 18 gamma-ray groups. Both of these libraries are discussed in Section M of the SCALE documentation.

Important input and output datasets prepared and generated for the studies reported in this document are included on a diskette attached to the back cover of this report. The files on the diskette are readable under DOS.

4.2 ISOTOPIC COMPOSITION OF SPENT FUEL

In many of the figures that follow, the time after discharge is shown on the abscissa. The times indicated are, loosely speaking, "logarithmic." Note, however, that the abscissa is not strictly a logarithmic scale. Rather, the times for which calculations were performed have been placed at equally spaced intervals.

Figures 2 and 3 show the uranium and neptunium isotopic contents for the uranium-burning and MOX-burning assemblies, respectively. The uranium assembly is charged with much more ^{235}U (the MOX fuel contained only uranium tails) and it burns more ^{235}U. As a direct consequence of burning ^{235}U, it will therefore contain more ^{236}U and ^{237}Np following discharge. However, for the longer decay times, the plutonium (MOX) assembly shows higher concentrations of ^{235}U, ^{236}U, and ^{237}Np, which is a consequence of the alpha decay of ^{239}Pu, ^{240}Pu, and ^{241}Am (from ^{241}Pu). The ^{237}Np can also come, via ^{237}U, from the decay of ^{241}Pu. The amount of ^{238}U is comparable in both assemblies.

Figures 4 and 5 illustrate the plutonium isotopic contents for the uranium- and MOX-burning assemblies, respectively. As regards the plutonium isotopes, there is about five times as much plutonium in the MOX fuel at discharge as there is in the uranium fuel at discharge. This difference is almost entirely due to the plutonium that was present in the beginning (the amount of ^{239}Pu generated during reactor operation is less than 1% of that present at discharge). However (although not clear from the ordinate scale in Fig. 5), the ^{239}Pu isotopic content of the MOX assembly was about 63% at discharge, whereas it was 93% in the fresh fuel. The ^{239}Pu isotopic content of discharged uranium-assembly fuel is 53.7%. If one looks at the concentration values in detail one will see that there continues to be a small amount of ^{241}Pu present out to 250,000 years even though it has a half-life of only 14.4 years (contrast with ^{238}Pu with a half-life of 87 years). The ^{241}Pu results from the decay of ^{245}Cm.

Figures 6 and 7 illustrate the americium and curium contents of the assemblies. All americium isotopes show higher concentrations in the MOX case relative to the uranium case (the ^{242m}Am content is negligible in the uranium-burning case and is not shown). This difference is due to the plutonium originally present in the fuel. However, the ^{244}Cm content is higher in the uranium case and by an amount that is about equal to the difference in total burn experienced by the two assemblies. Of course, the ^{244}Cm has a short half-life (18.1 years), and it decays quickly.

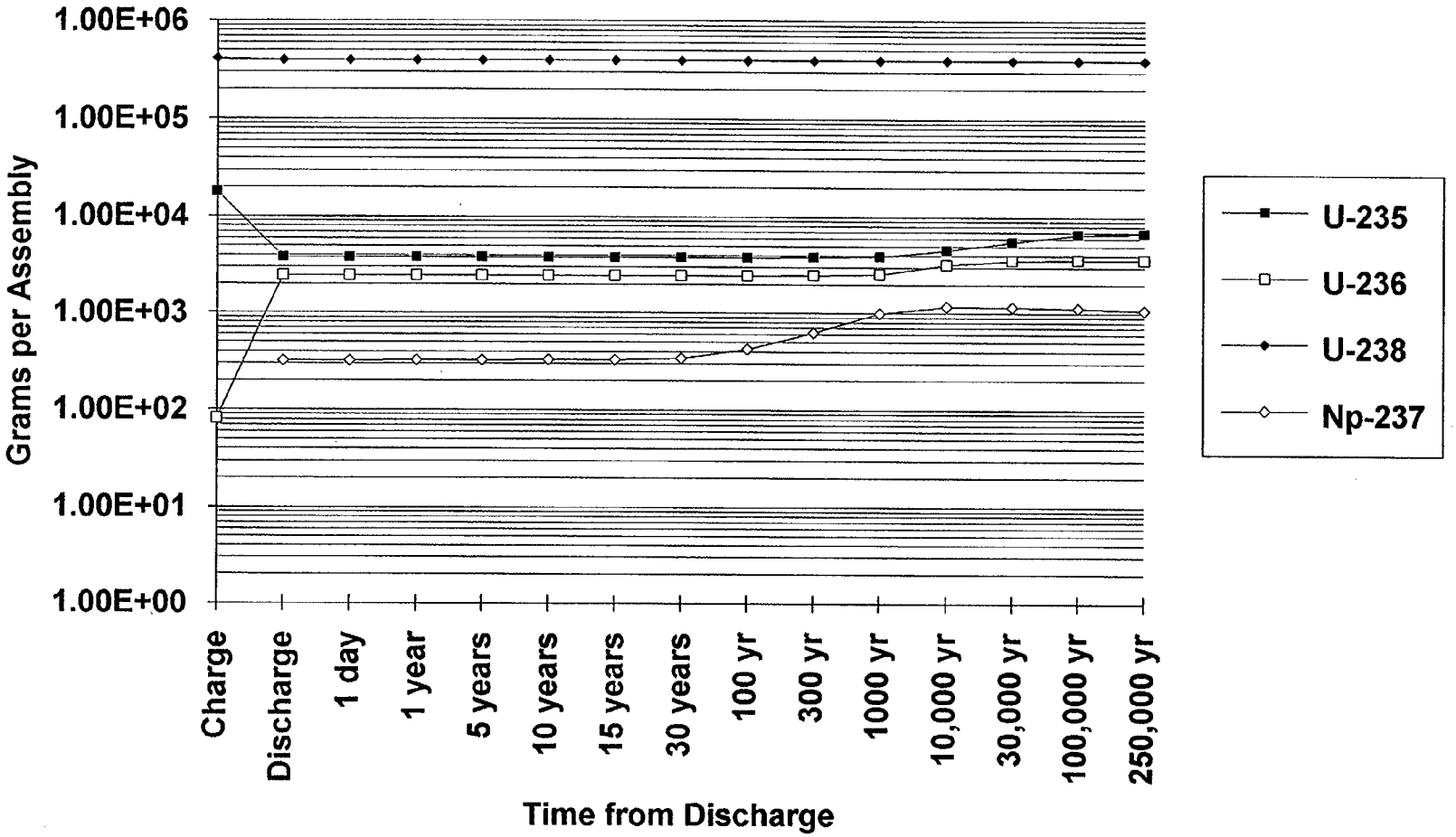

Fig. 2. The uranium and neptunium content of a uranium-fueled assembly following discharge.

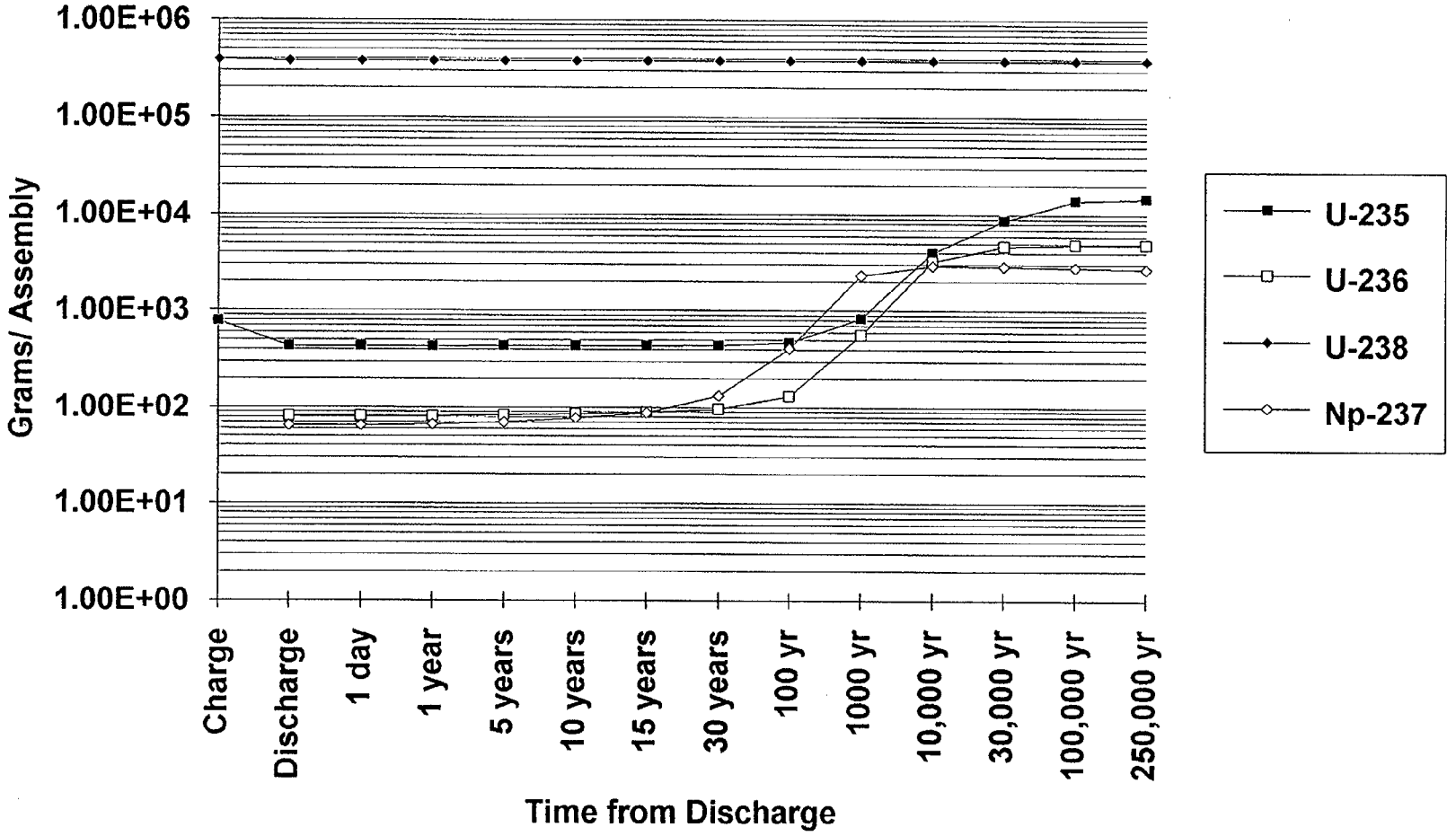

Fig. 3. The uranium and neptunium content of a MOX-fueled assembly following discharge.

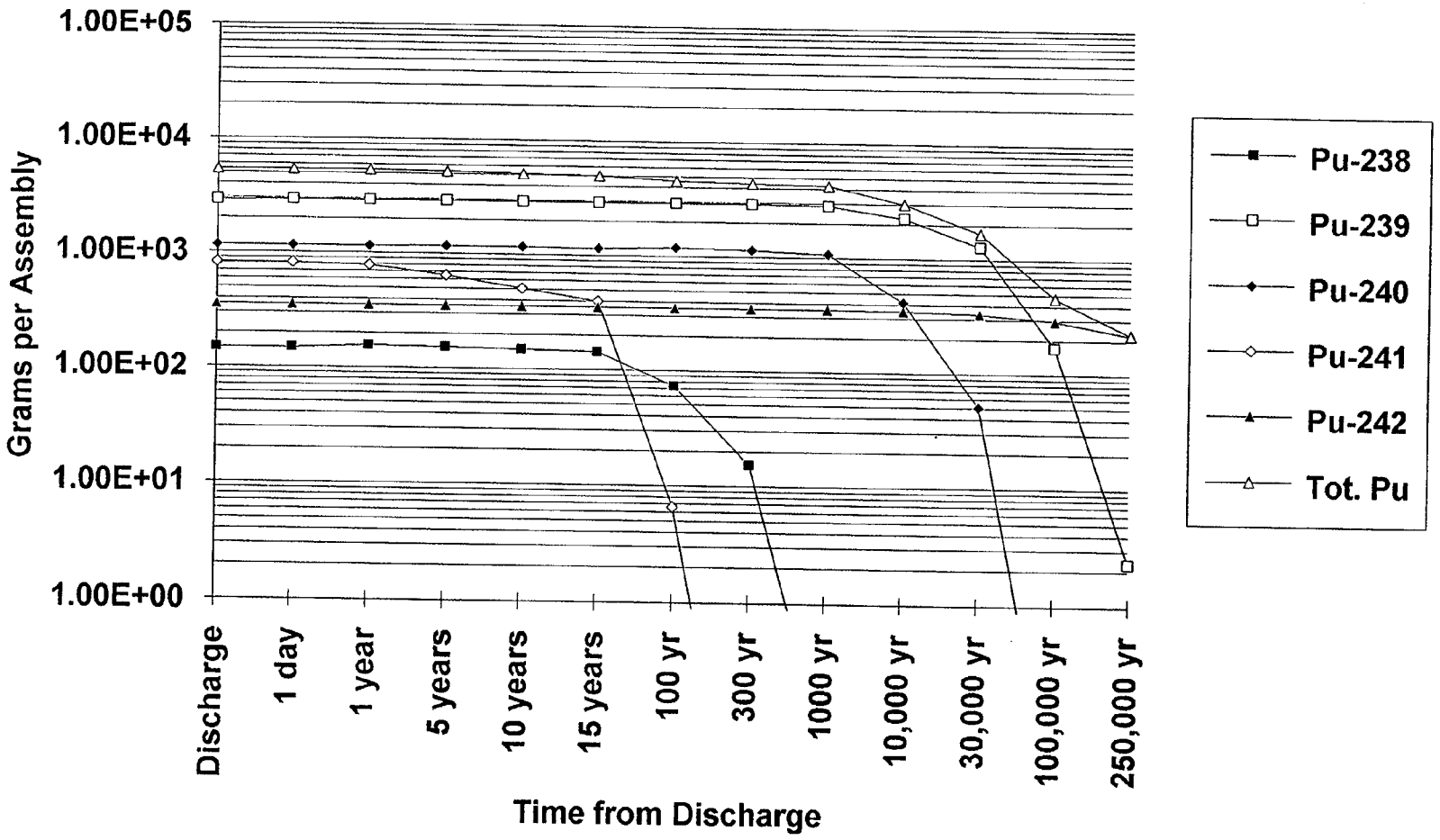

Fig. 4. The plutonium content of a uranium-fueled assembly following discharge.

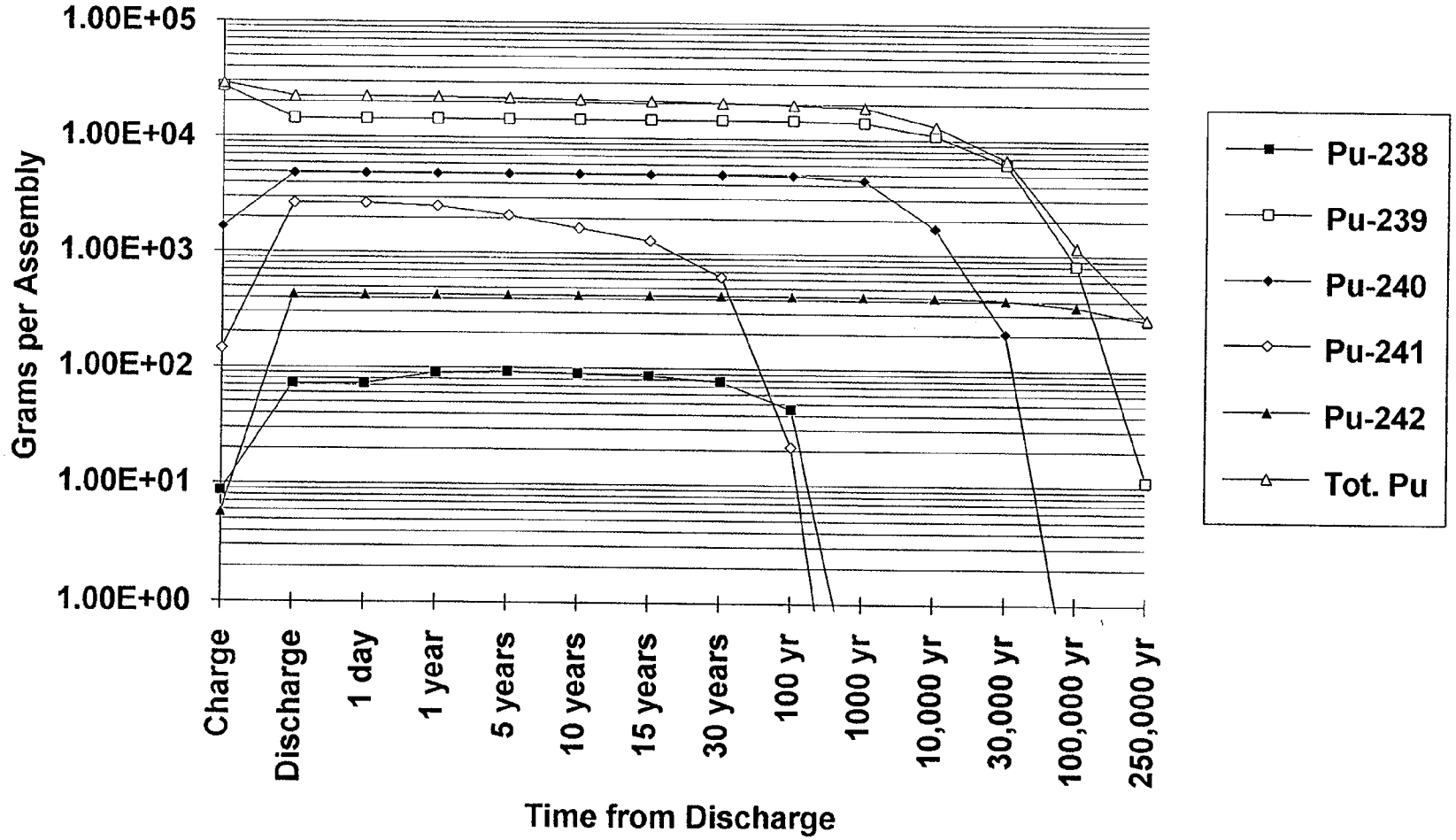

Fig. 5. The plutonium content of a MOX-fueled assembly following discharge.

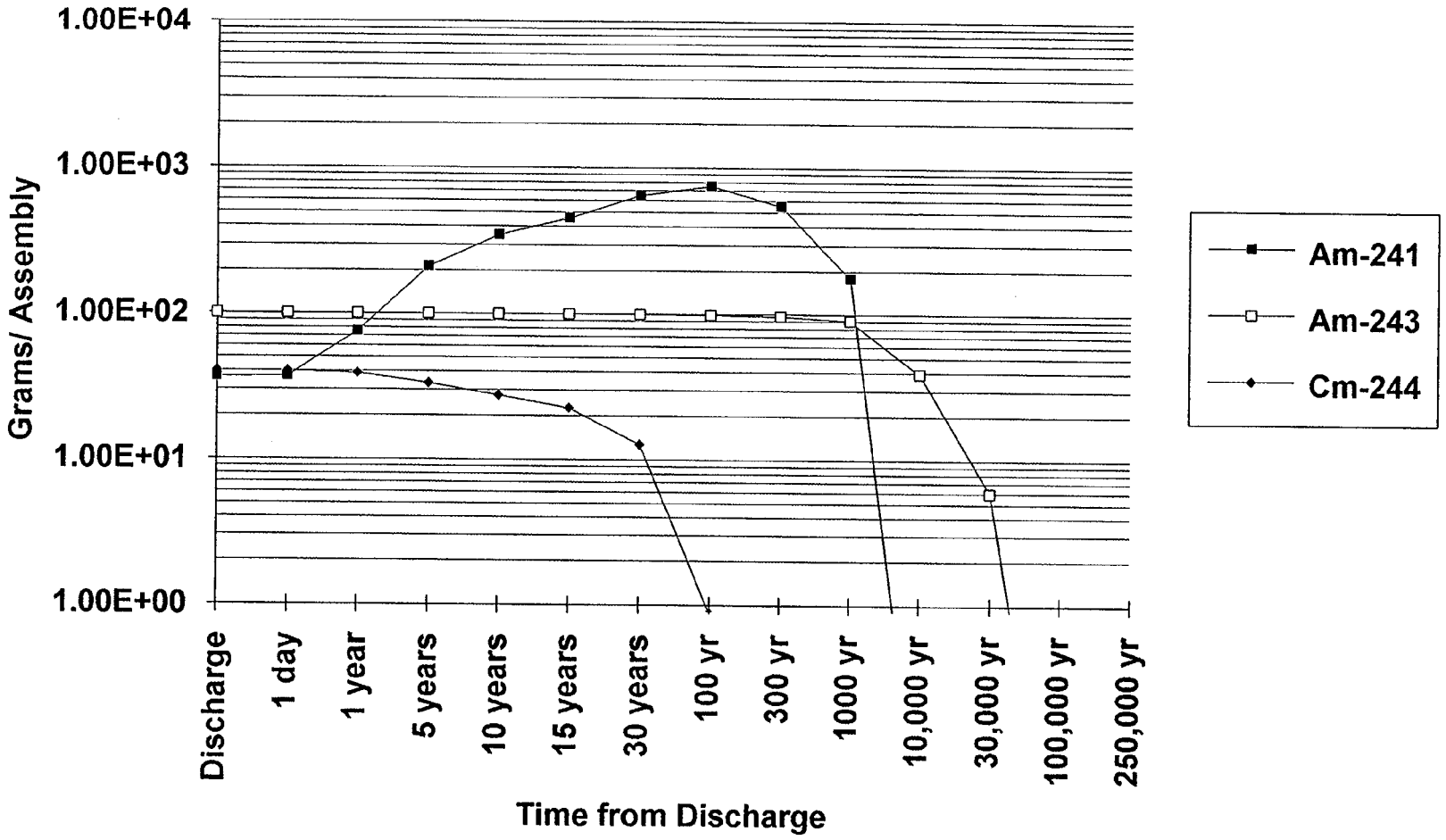

Fig. 6. The americium and curium content of a uranium-fueled assembly following discharge.

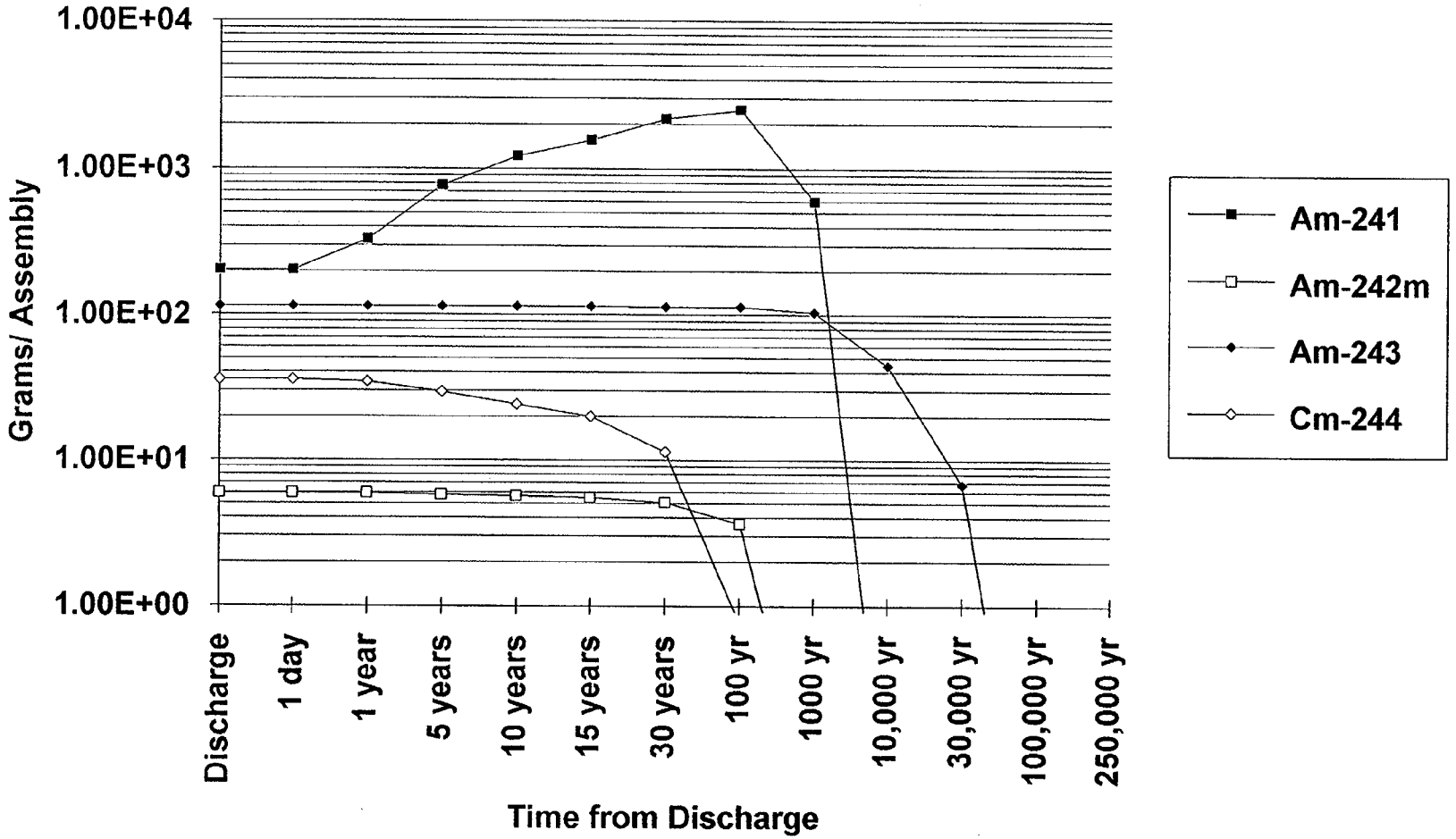

Fig. 7. The americium and curium content of a MOX-fueled assembly following discharge.

4.3 ACTIVITIES

The activities in a MOX-fueled assembly at various times following discharge are shown in Fig. 8. Most of the contribution to activity comes from actinides and fission products. The light-element contribution is on the order of, or somewhat less than, 1%. If all else were equal, the light-element contribution to the activity would be expected to be proportional to the total burnup. However, as specified, the assemblies contained different amounts of zirconium. These different quantities of zirconium in the assemblies and, hence, the different amounts of zirconium and niobium isotopes following discharge, constitute most of the variations in light-element activity. Figure 9 shows activity levels from the uranium-fueled assembly at various times following discharge. The results are not greatly different, but (apart from times immediately following discharge) it is apparent that more activity results from actinides in the MOX case.

A major contributor to the light-element activity is ^{60}Co. The amount of ^{60}Co at discharge depends on the amount of cobalt (100% ^{59}Co) in the structural materials of the assembly. The cobalt content of both the MOX- and uranium-fueled assemblies was the same. It was set at a value that is considered typical for a PWR.

Fission-product activities are comparable but with the uranium case giving somewhat higher values than the plutonium case. However, the ratio between the two cases is not the same as the ratio of the burnups, although this might be expected for the fission products. On the other hand, the activity ratio for ^{137}Cs is equal to the ratio of burnups. Since ^{137}Cs is a long-lived fission product and is near the top of the heavy-fragment peak, this result is as expected. Those parts of the differences in activities not accounted for by the differences in burnups are likely due to any or all of the following reasons:

1. the concentration of shorter-lived species is affected by the details of the burn history;

2. the somewhat different distribution of actinides gives a different distribution of fission products; and

3. for fission products whose yields are low, the estimates of those yields will be subject to considerable uncertainty.

Overall activity should be considered as a gross assessment of spent fuel characteristics. Activity includes alpha, beta, and gamma radiation, and consequently the significance of a given amount of activity in terms of its effects is dependent on the source of that activity and the combination of types of radiation involved. The actinides will be responsible primarily for the alpha emissions and some spontaneous fission which, in turn, means neutron emission. Light elements (i.e., structural materials) give rise to beta and gamma emissions and in particular ^{60}Co gamma radiation. Fission products produce the majority of the beta and gamma radiation. Among the fission products, ^{90}Sr is a significant beta emitter, with ^{137}Cs and ^{134}Cs being significant gamma emitters.

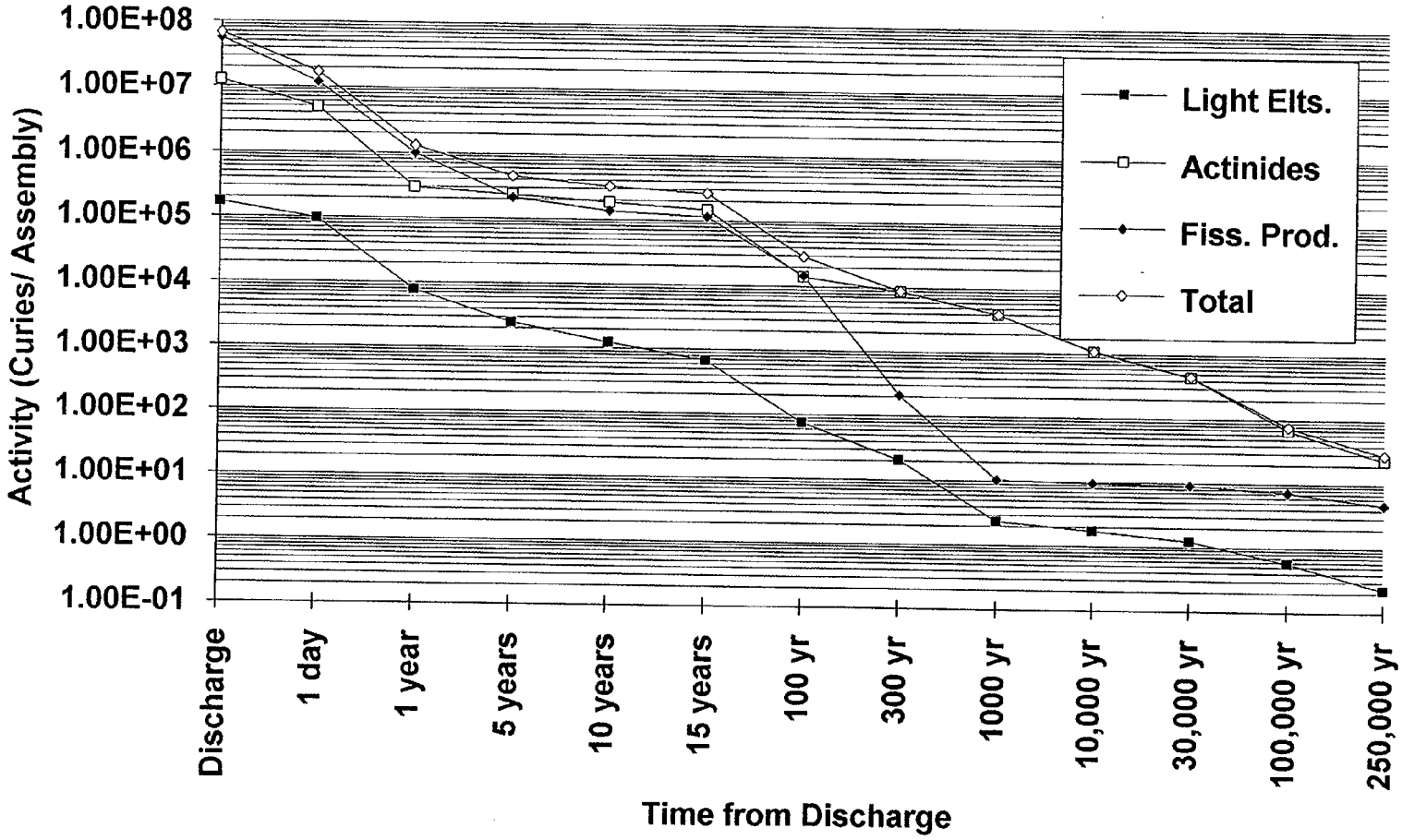

Fig. 8. Total activity of a MOX-fueled assembly following discharge.

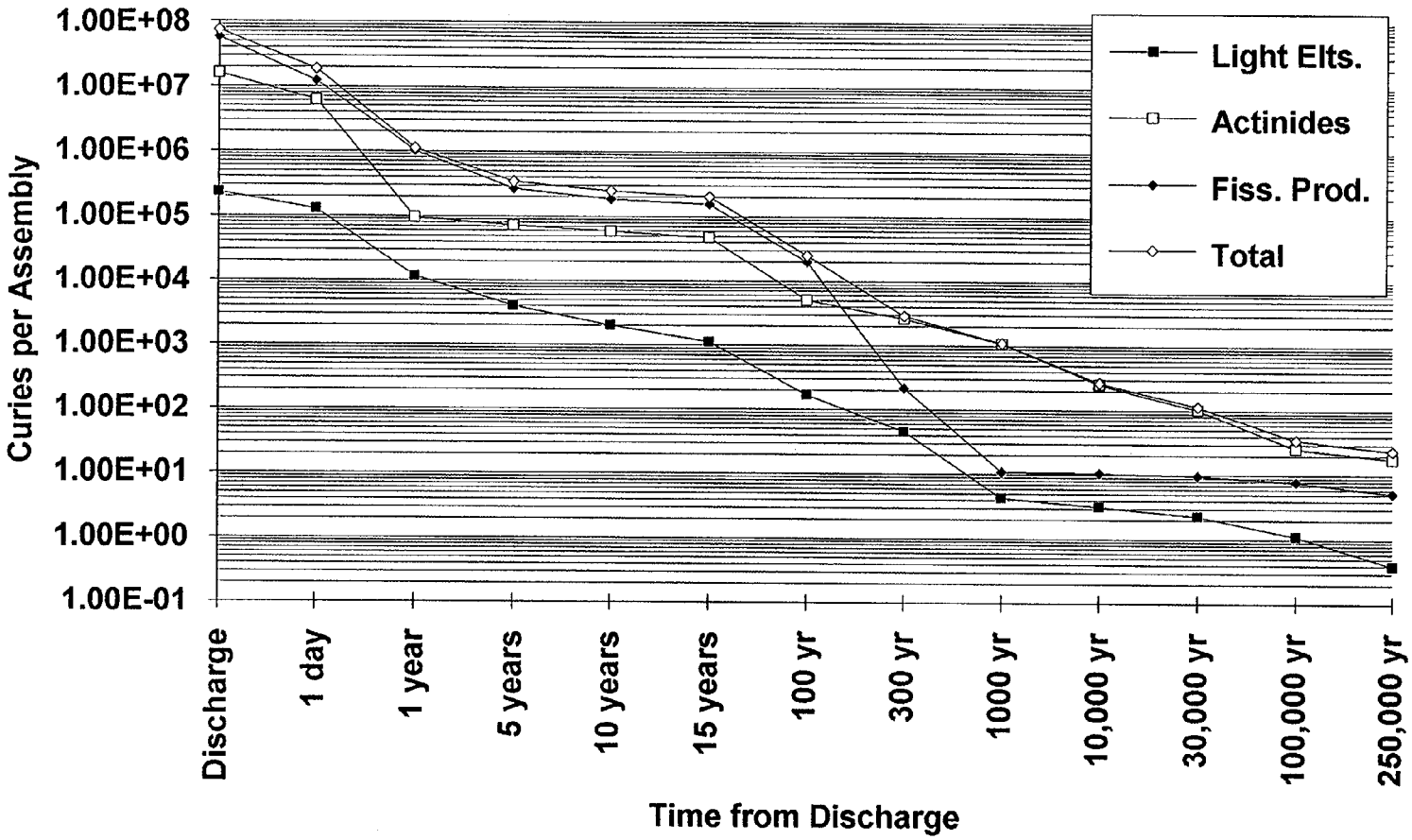

Fig. 9. Total activity of a uranium-fueled assembly following discharge.

Considering just raw activities, these levels are higher in the plutonium-burning case beginning at a few hundred years and going out to 100,000 years or so. In parts of this time frame, the activity is up to a factor of 4 higher for the plutonium case and is actually due to the higher amount of plutonium present. At times shorter than a few hundred years, the fission-product activity dominates, and it is somewhat greater in the uranium case due to the higher total burnup.

4.4 GAMMA FLUX

The gamma radiation from the spent fuel comes mostly from the fission products, with ^{60}Co from the structural materials also producing significant gamma radiation in the early stages after discharge (the half-life of ^{60}Co is 5.3 years). Cobalt-60 gamma lines are at 1.17 and 1.33 MeV. Two of the very important fission products contributing to the gamma flux are ^{134}Cs (605 and 796 keV) and ^{137}Cs (662 keV).

Gamma-ray spectra are shown in Figs. 10 through 14. The energy group structure used to produce the spectra in Figs. 10 through 14 is shown in Table 3. These groups are known as the SCALE 18-group gamma structure. For all but a small number of the energy groups there is negligible flux in evidence in the figures. Note that the group with an upper energy of 1.0 MeV is group number 11, and the groups with noticeable flux can be identified with reference to this (group numbers increase with decreasing energy). Thus the ^{137}Cs 662-keV line would contribute to group 12, for instance.

Figures 10 through 14 show the dominance of ^{137}Cs as a gamma-ray source. Figure 10 shows the gamma flux spectrum at 1 m from an unshielded MOX assembly 1 day after discharge. Figure 11 is the corresponding plot for a uranium-fueled assembly. The noteworthy point in comparing Figs. 10 and 11 is that there is no difference in the form of the spectra and that the differences in intensity are about equal to the differences in total burn. Figure 12 is for the MOX assembly 5 years after discharge, and Fig. 13 is for the MOX assembly 100 years following discharge. Figure 14 shows the gamma flux at 1 m from a Transnuclear TN-24P shielding cask[7] containing 11 MOX assemblies at 5 years from discharge. The attenuation introduced by the shielding cask is obvious from the intensity relative to that for the unshielded assemblies.

In these various gamma-ray spectra, the ^{134}Cs contribution will be seen in group 12 but is overshadowed by the ^{137}Cs contribution. The ^{134}Cs contribution is in evidence only in the earlier stages (half-life of 2.07 years); the ^{137}Cs contribution is much more lasting, having a half-life of 30 years.

Evidence supports the presence of ^{60}Co for the earlier times (it contributes to groups 9 and 10). The half-life of ^{60}Co is 5.3 years. As noted earlier, the contribution depends on the amount of cobalt (100% ^{59}Co) in the original structural materials of the assembly. Cobalt is a contaminant in nickel and therefore is present in alloys that contain nickel. In these studies, we have assumed 0.033 kg of cobalt per assembly with the understanding that the actual value can be quite variable. The subject of the elemental composition of reactor assemblies is addressed by Hermann et al.[6] and in references quoted therein.

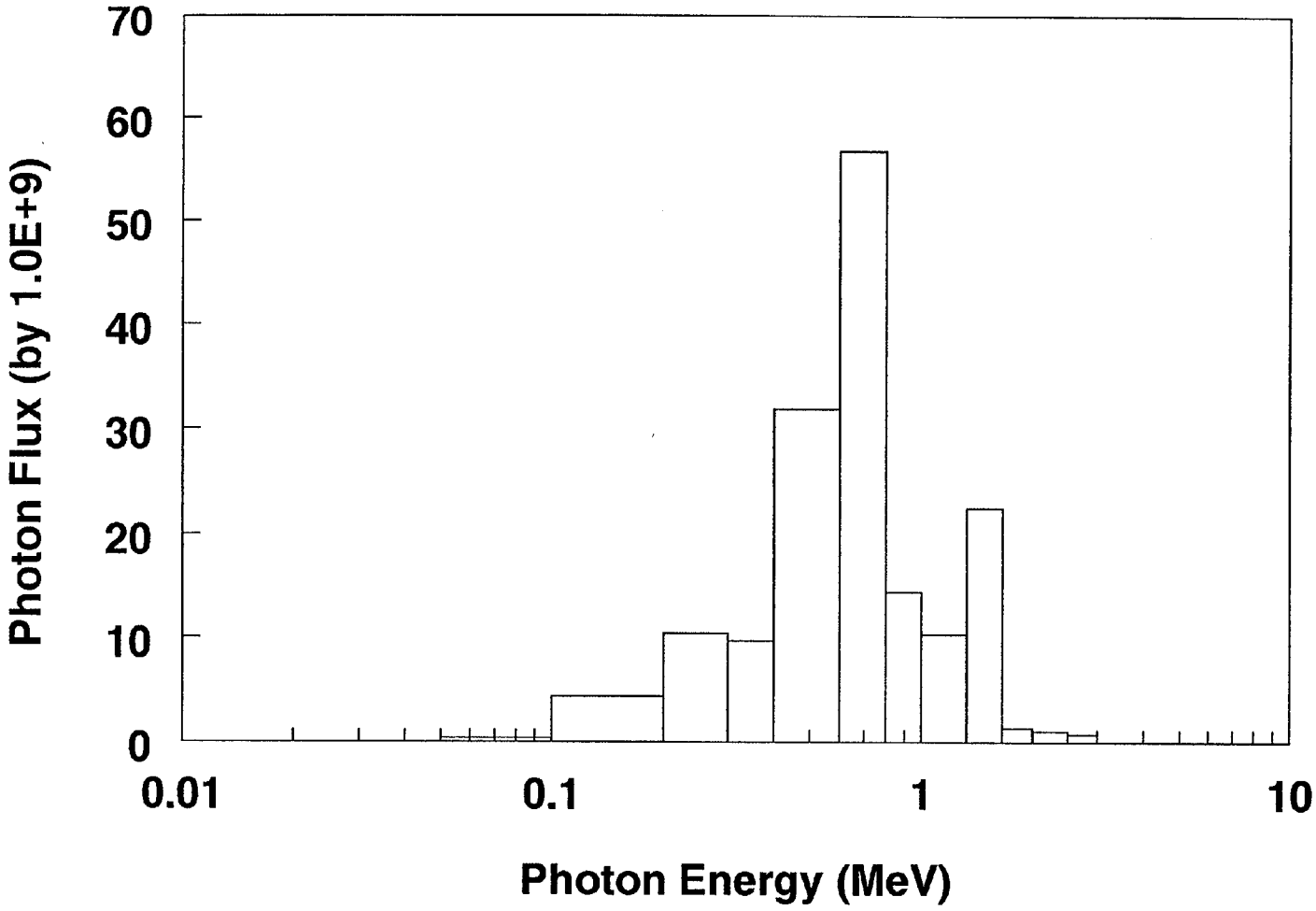

Fig. 10. The gamma flux at 1 m from the side of an unshielded MOX assembly 1 d after discharge.

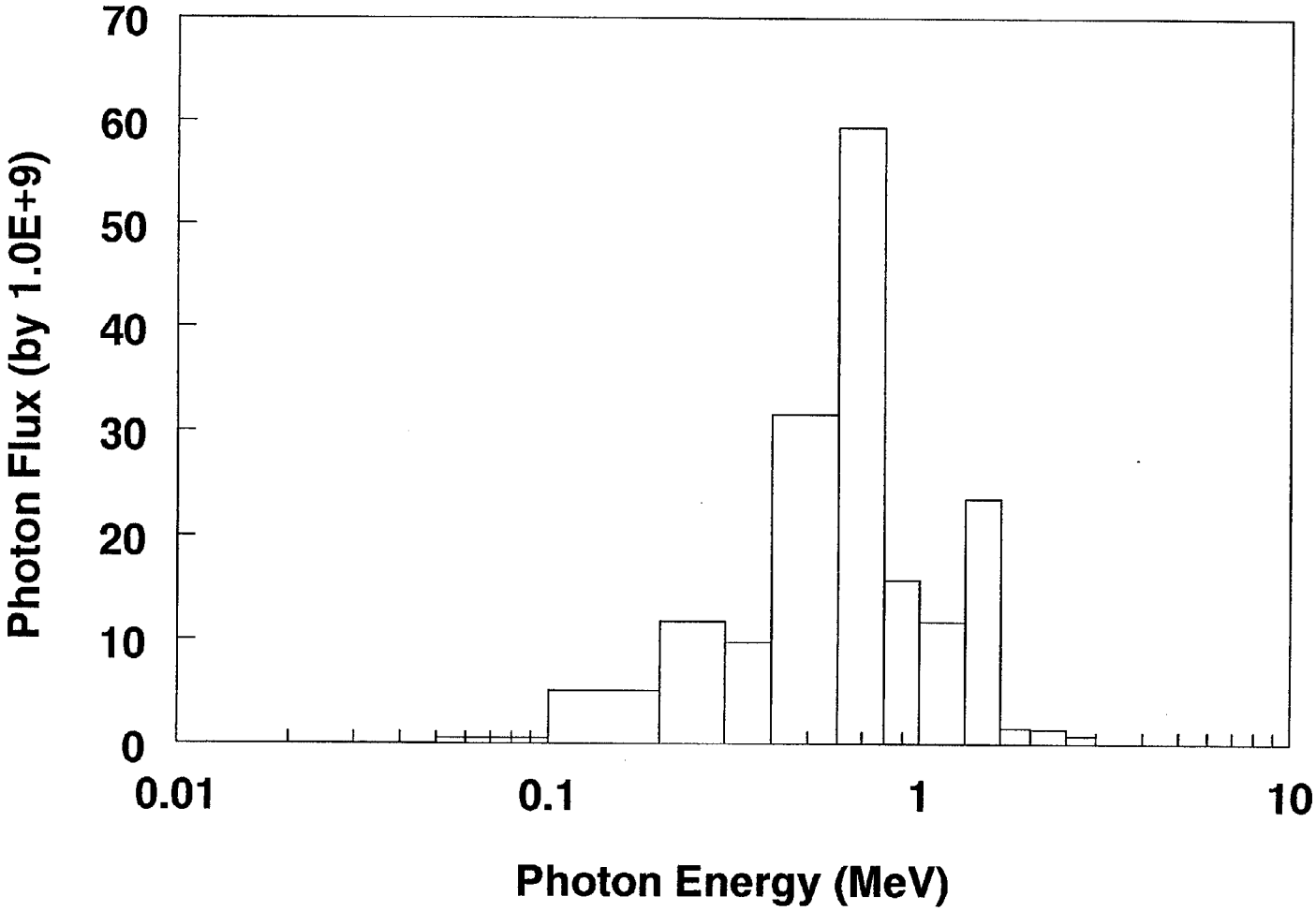

Fig. 11. The gamma flux at 1 m from the side of an unshielded uranium assembly 1 d after discharge.

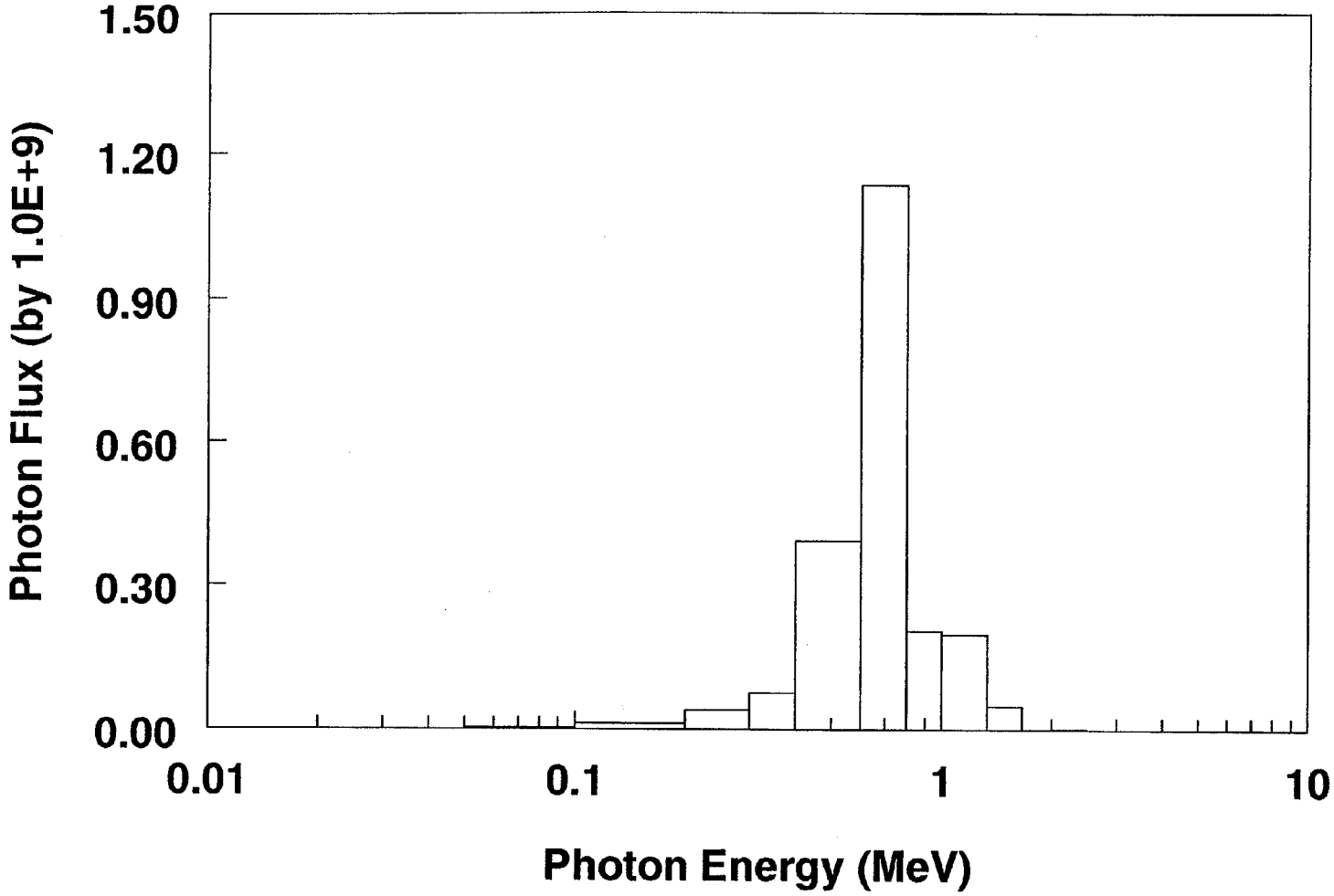

Fig. 12. The gamma flux at 1 m from the side of an unshielded MOX assembly 5 years after discharge.

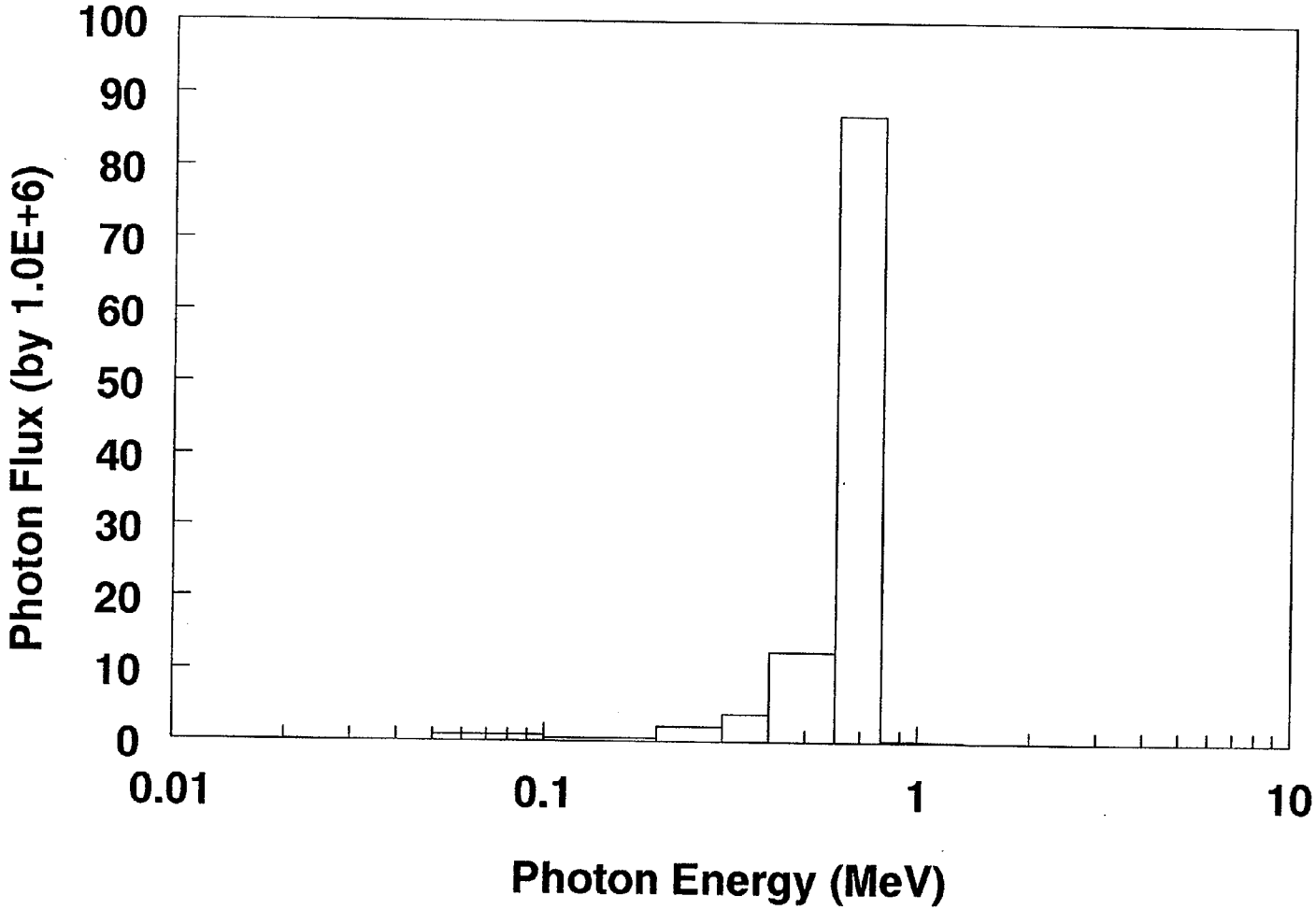

Fig. 13. The gamma flux at 1 m from the side of an unshielded MOX assembly 100 years after discharge.

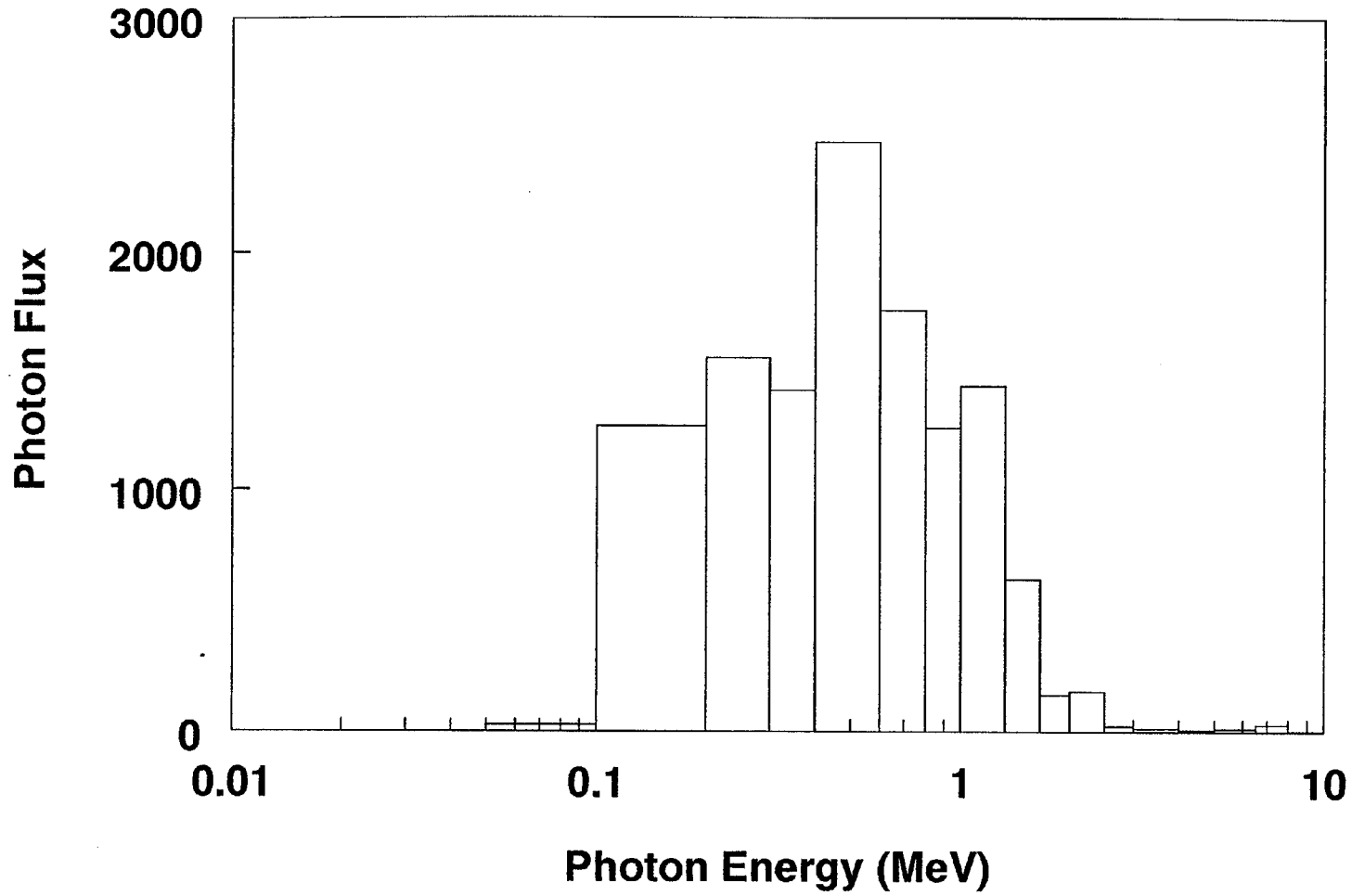

Fig. 14. The gamma flux at 1 m from the side of a cask containing 11 MOX-fueled assemblies 5 years after discharge.

Table 3. Energy group structure for gamma dose calculations

SCALE 18-group gamma structure	Upper energy (MeV)
1	10.0
2	8.0
3	6.5
4	5.0
5	4.0
6	3.0
7	2.5
8	2.0
9	1.66
10	1.33
11	1.0
12	0.8
13	0.6
14	0.4
15	0.3
16	0.2
17	0.1
18	0.05
Lower energy bound	0.01

Returning again to the effect of a shielding cask on the radiation (Fig. 14), when one looks at the gamma radiation at 1 m from a cask containing 11 assemblies one, of course, sees that there is significant attenuation. Also, the radiation outside the cask contains a considerable gamma flux due to Compton scattering in the cask material and furthermore, most of the radiation below 100 keV has been absorbed by the cask.

4.5 DECAY HEAT FROM SPENT FUEL

Figure 15 shows the decay heat generated by a spent MOX fuel assembly. The contributions from actinides, fission products, and light elements are shown as is the total decay heat. Decay heat as calculated is the total amount of decay energy in joules per second generated by the spent fuel. Whether or not this is evident as heat in the immediate vicinity of the spent fuel will depend on the composition of the assembly and any shielding that may be present. The utility of using decay heat to characterize an assembly lies in the assumption that there is sufficient shielding such that the heat will manifest itself locally. In the early stages following discharge, it is mostly the fission products that contribute to the decay heat. In the time frame of 10 to 15 years beyond discharge, however, the contribution of the actinides begins to dominate.

The results of decay heat calculations in the uranium-assembly case are shown in Fig. 16. These results are not greatly different than those in the MOX case, and the differences that do exist are hardly noticeable when comparing Figs. 15 and 16. The fission-product contribution to the decay heat is greater in the case of the uranium assembly, a fact that is commensurate with the greater burnup of that assembly. Immediately following discharge, the contribution of the actinides to the decay heat is also greater for the uranium assembly. However, at all other calculated times, the actinide contribution is greater in the case of the MOX assembly. Essentially, one is seeing the effects of the plutonium in the MOX fuel. The larger actinide contribution immediately following discharge in the case of the uranium assembly is from the somewhat greater amount of short-lived actinides that result from the larger burnup experienced by that assembly.

In regard to the storage of spent fuel assemblies and the use of wet vs dry storage arrangements, the results from the MOX and uranium assemblies are not very different. Just after discharge, one sees values in the range of 70 to 80 MW per assembly, which drops to around 5 kW after 1 year. At some hundreds of years following discharge the value drops to several hundred watts. At 10 years, for instance, the MOX and uranium assemblies give values of 730 and 790 W, respectively.

4.6 DOSE RATES

Figure 17 shows the ratios of the gamma dose rates in rems/h for the uranium-fueled assembly vs the MOX-fueled assembly. These ratios are for dose rates at 1 m from a bare assembly. Dose rates from the bare assemblies (and on the outside of casks containing assemblies) are comparable for both the MOX and the uranium cases. The differences vary with time and for a combination of reasons. But, broadly speaking, differences come about because of the different actinides that are present and because of the larger burnup in the case of the uranium assembly. Examining Fig. 17, one sees that the differences are within the range expected from the difference in burnup. Recalling the

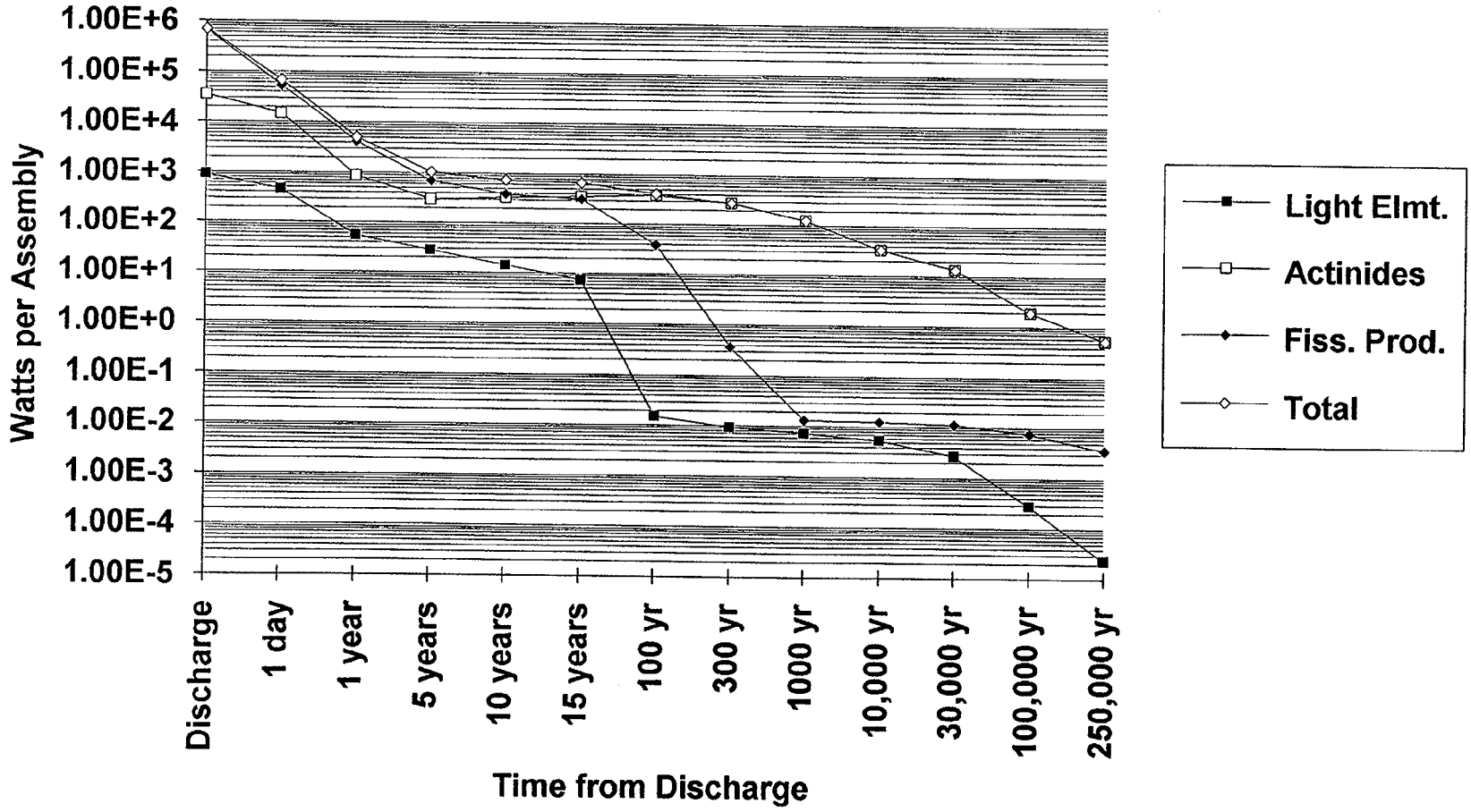

Fig. 15. Decay heat from a MOX-fueled assembly following discharge.

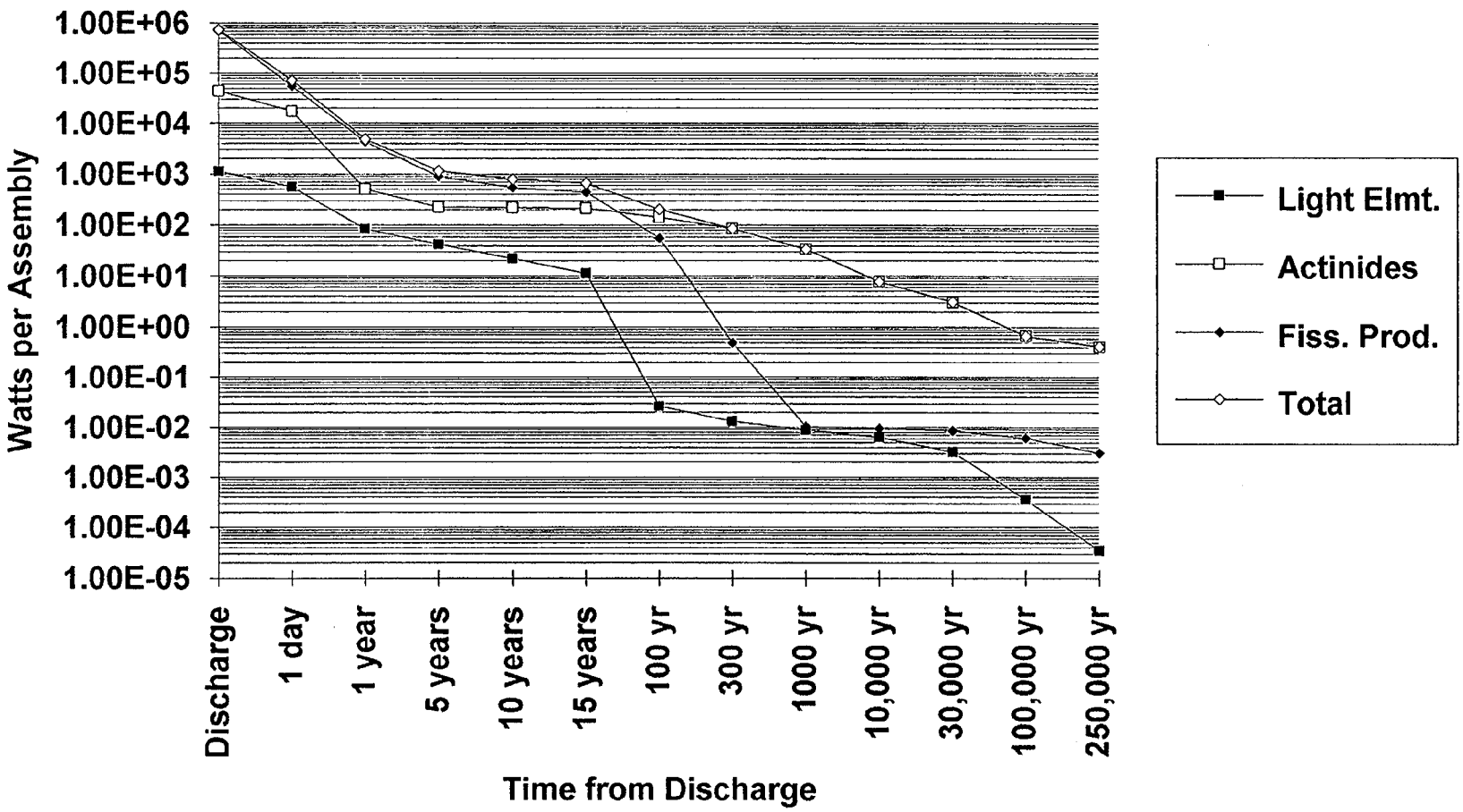

Fig. 16. Decay heat from a uranium-fueled assembly following discharge.

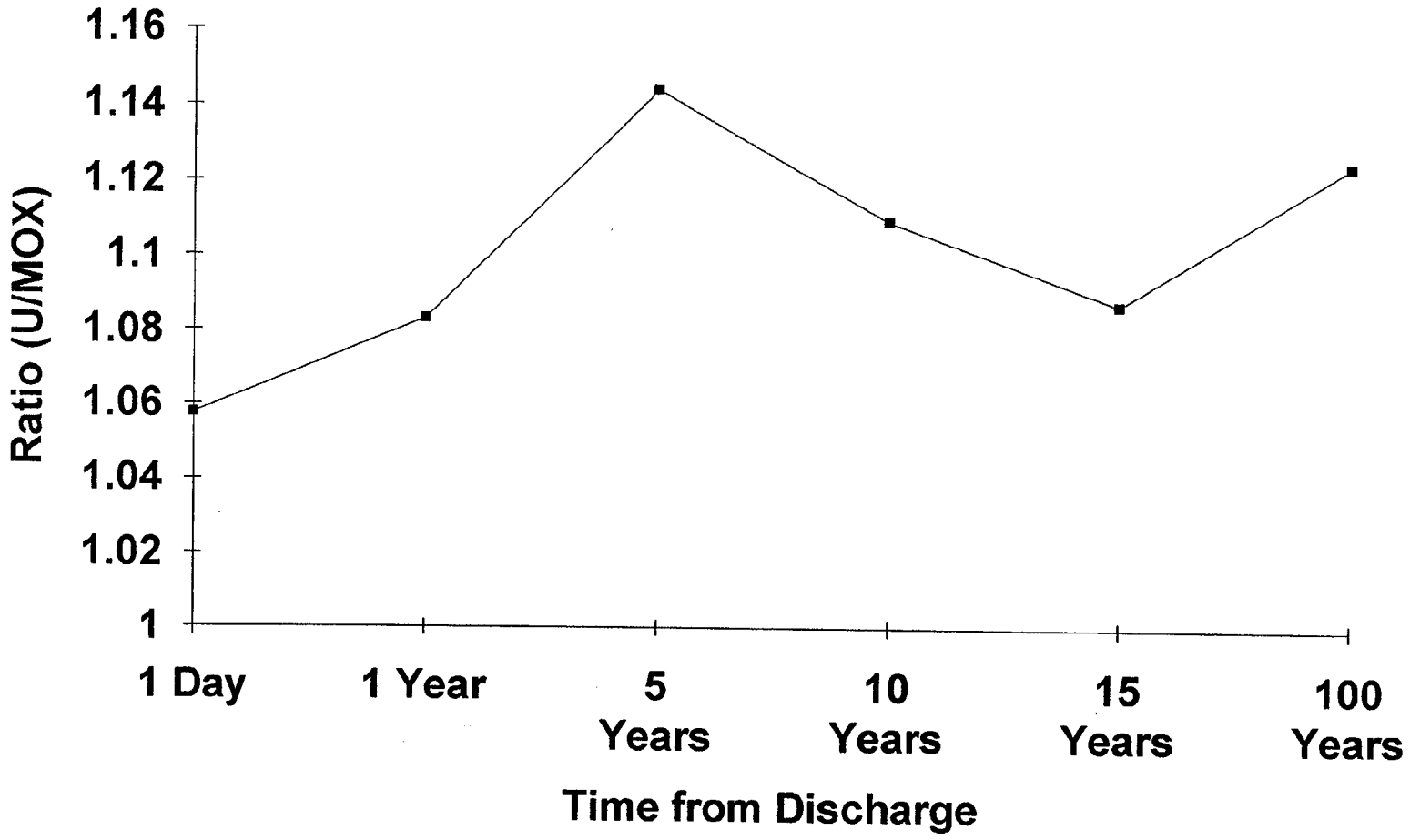

Fig. 17. The ratio of gamma dose rates (uranium-fueled to MOX-fueled) at 1 m from bare assemblies.

above discussion of gamma-ray spectra, the prominent contributors were ^{134}Cs and ^{137}Cs from the fission products and ^{60}Co from the structural materials. One would expect that to a first approximation, the concentrations of these nuclides will be proportional to burnup, and in the case of the ^{60}Co, the concentration will also be dependent on the amount of cobalt in the original structural material.

The absolute values of the gamma dose rates for the MOX fuel cycle are shown in Fig. 18. Beyond a few hundred years, the values are quite small. The data shown are for a MOX assembly, but, for the uranium-fueled assembly the form of the curve is the same. Note that the dose rate is on the order of 150 rem/h at 100 years following discharge.

4.7 SEVERE ACCIDENT ANALYSES

Design-basis accidents usually involve destruction of the fuel by some mechanism with consequent release to the environment of various fission products and actinides. One question of concern to the plutonium disposition program is whether the consequences of a severe accident with MOX fuel exceeds the consequences of a similar accident with low-enriched uranium fuel. Even though the analysis of such an accident is beyond the scope of these studies, input to severe accident studies can be obtained from ORIGEN analyses.

The activities for selected nuclides commonly input to accident analyses are shown in Table 4. Data for both MOX and uranium cycles are shown at the time of discharge. Some obvious differences are observed between the two cases.

4.8 CRITICALITY SAFETY FOR GEOLOGIC REPOSITORY

Assessment of repository safety involves analyses covering time periods thousands of years into the future. Even though actinide concentrations have been presented above, criticality analyses for a repository include selected nuclides that have significant absorption cross sections (i.e., they are good neutron poisons). Estimates of the quantities of these nuclides for the System 80+ fuel cycles can be obtained from ORIGEN calculations, and they are listed in Table 5, where the values refer to the time of discharge. Data for both the MOX and uranium cases are provided. Again, some obvious differences can be seen between the two cases.

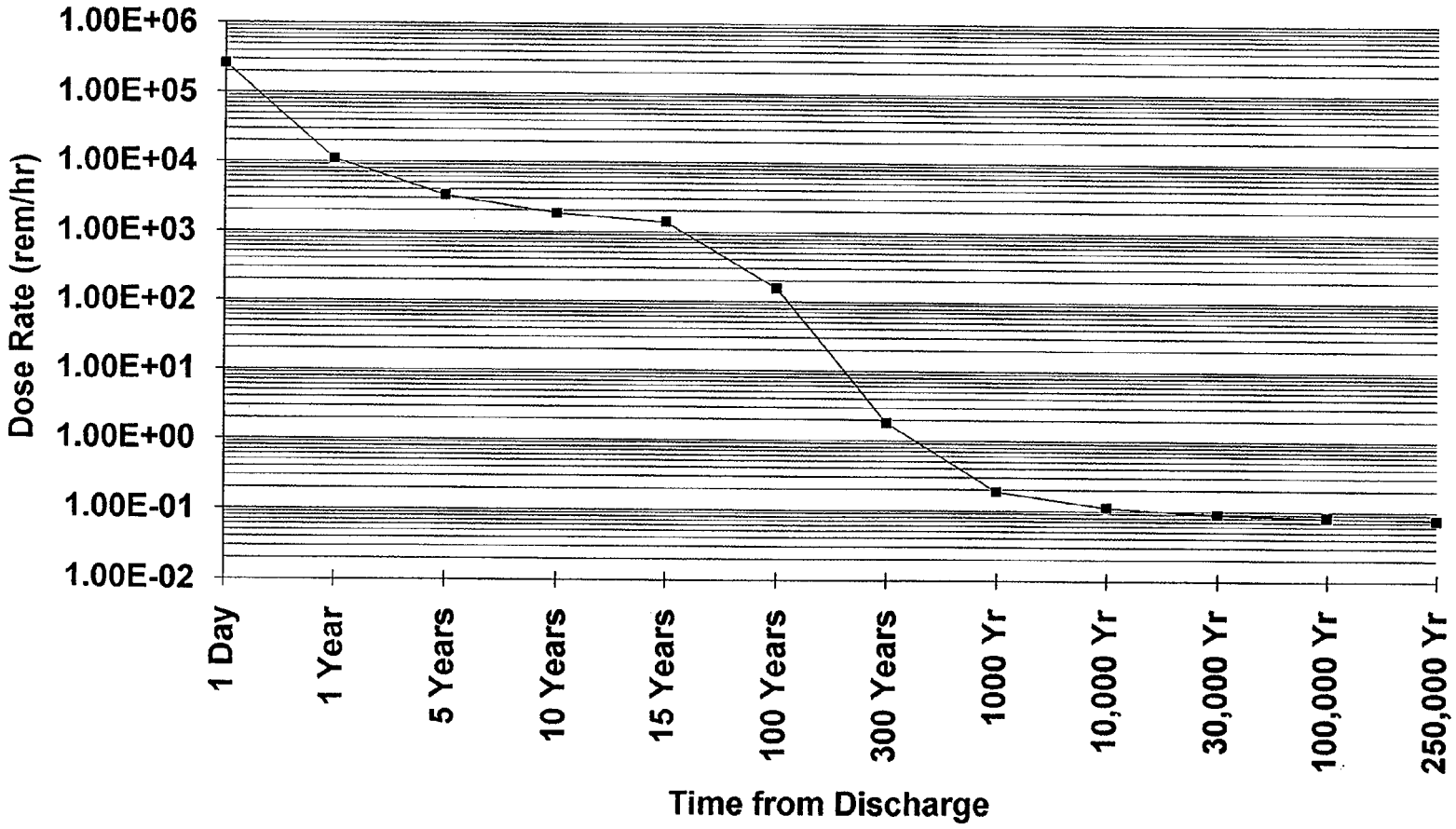

Fig. 18. The gamma dose rate at 1 m from the side of a bare MOX-fueled assembly following discharge.

Table 4. Comparison of principal activity sources at discharge from System 80+ for MOX and low-enriched uranium fuel assemblies

Nuclide	Activity (Ci)		Ratio (MOX/U)
	MOX	LEU	
^{241}Am	6.96E+02	1.25E+02	5.57
^{140}Ba	5.44E+05	5.79E+05	0.94
^{14}C	3.27E−01	7.51E−01	0.44
^{141}Ce	5.00E+05	5.32E+05	0.94
^{143}Ce	4.29E+05	4.80E+05	0.89
^{144}Ce	3.51E+05	4.36E+05	0.81
^{242}Cm	8.05E+04	3.56E+04	2.26
^{244}Cm	2.87E+03	3.25E+03	0.88
^{58}Co	5.65E+03	5.15E+03	1.10
^{60}Co	3.38E+03	5.28E+03	0.64
^{134}Cs	7.03E+04	9.94E+04	0.71
^{134m}Cs	1.31E+04	1.84E+04	0.71
^{136}Cs	4.17E+04	3.00E+04	1.39
^{137}Cs	5.70E+04	6.47E+04	0.88
^{3}H	2.76E+02	2.84E+02	0.97
^{131}I	3.43E+05	3.30E+05	1.04
^{132}I	4.90E+05	4.79E+05	1.02
^{133}I	6.52E+05	6.65E+05	0.98
^{135}I	6.24E+05	6.38E+05	0.98
^{85}Kr	2.69E+03	5.02E+03	0.54
^{85m}Kr	5.07E+04	7.02E+04	0.72
^{88}Kr	1.30E+05	1.92E+05	0.68
^{140}La	5.55E+05	6.00E+05	0.93
^{141}La	4.96E+05	5.26E+05	0.94
^{99}Mo	5.89E+05	6.06E+05	0.97
^{95}Nb	4.56E+05	5.26E+05	0.87
^{95m}Nb	5.21E+03	5.89E+03	0.88
^{147}Nd	2.05E+05	2.16E+05	0.95
^{238}Np	3.48E+04	2.07E+05	0.12
^{143}Pr	4.21E+05	4.78E+05	0.88
^{238}Pu	1.24E+03	2.55E+03	0.49
^{239}Pu	8.93E+02	1.79E+02	4.99
^{240}Pu	1.10E+03	2.64E+02	4.17
^{241}Pu	2.76E+05	8.52E+04	3.24
^{86}Rb	3.72E+02	8.36E+02	0.44
^{105}Rh	4.99E+05	3.85E+05	1.30

Table 4 (continued)

	Activity (Ci)		
Nuclide	MOX	LEU	Ratio (MOX/U)
^{105m}Rh	1.45E+05	1.16E+05	1.25
^{103}Ru	6.44E+05	5.60E+05	1.15
^{105}Ru	5.10E+05	4.10E+05	1.24
^{106}Ru	3.74E+05	2.57E+05	1.46
^{127}Sb	3.86E+04	3.09E+04	1.25
^{129}Sb	1.22E+05	1.09E+05	1.12
^{89}Sr	1.69E+05	2.65E+05	0.64
^{90}Sr	2.00E+04	4.45E+04	0.45
^{91}Sr	2.45E+05	3.43E+05	0.71
^{92}Sr	2.90E+05	3.75E+05	0.77
^{99m}Tc	5.22E+05	5.39E+05	0.97
^{127}Te	3.84E+04	3.06E+04	1.25
^{127m}Te	6.69E+03	5.23E+03	1.28
^{129}Te	1.17E+05	1.04E+05	1.13
^{129m}Te	2.41E+04	2.11E+04	1.14
^{132}Te	4.76E+05	4.70E+05	1.01
^{131m}Xe	4.47E+03	4.76E+03	0.94
^{133}Xe	6.55E+05	6.68E+05	0.98
^{133m}Xe	2.16E+04	2.13E+04	1.01
^{135}Xe	4.80E+05	2.33E+05	2.06
^{135m}Xe	1.52E+05	1.43E+05	1.06
^{90}Y	2.03E+04	4.70E+04	0.43
^{91}Y	2.46E+05	3.54E+05	0.69
^{91m}Y	1.42E+05	1.99E+05	0.71
^{92}Y	2.91E+05	3.78E+05	0.77
^{93}Y	2.45E+05	2.95E+05	0.83
^{95}Zr	4.58E+05	5.42E+05	0.85
^{97}Zr	4.86E+05	5.46E+05	0.89

Table 5. Concentrations of nuclides of interest for criticality safety

Nuclide	Grams per assembly		Ratio (MOX/U)
	MOX	LEU	
^{16}O	5.63E+04	5.70E+04	0.99
^{95}Mo	2.96E+02	4.12E+02	0.72
^{101}Ru	4.27E+02	4.64E+02	0.92
^{99}Tc	4.04E+02	4.58E+02	0.88
^{103}Rh	3.71E+02	2.50E+02	1.48
^{109}Ag	9.50E+01	5.10E+01	1.86
^{143}Nd	4.25E+02	4.66E+02	0.91
^{145}Nd	3.04E+02	3.94E+02	0.77
^{147}Sm	4.65E+01	5.23E+01	0.89
^{149}Sm	4.96E+00	1.41E+00	3.52
^{150}Sm	1.57E+02	1.81E+02	0.87
^{151}Sm	2.55E+01	1.03E+01	2.48
^{152}Sm	7.94E+01	7.21E+01	1.10
^{153}Eu	7.38E+01	7.52E+01	1.02
^{155}Gd	2.08E-01	5.13E-02	4.05
^{235}U	4.32E+02	3.82E+03	0.11
^{236}U	8.13E+01	2.44E+03	0.03
^{238}U	3.77E+05	3.91E+05	0.96
^{237}Np	6.50E+01	3.19E+02	0.20
^{238}Pu	7.24E+01	1.49E+02	0.49
^{239}Pu	1.44E+04	2.89E+03	4.98
^{240}Pu	4.85E+03	1.16E+03	4.18
^{241}Pu	2.67E+03	8.23E+02	3.34
^{242}Pu	4.31E+02	3.56E+02	1.21
^{241}Am	2.03E+02	3.66E+01	5.55
^{242m}Am	5.91E+00	8.66E-01	6.82
^{243}Am	1.14E+02	9.97E+01	1.14
^{245}Cm	2.11E+00	1.88E+00	1.12

5. CONCLUSIONS AND OBSERVATIONS

The calculations reported here refer to the nuclide inventories in assemblies containing spent MOX fuel. Similar assemblies containing only conventional uranium fuel have also been discussed for comparison purposes. Besides the nuclide inventories themselves, important issues regarding safety, transportability, radiological, and other hazards have been discussed. These results provide a technical background on which to base decisions on the best method for plutonium disposition.

For the gross hazard parameters defining a spent fuel assembly (dose rate, decay heat, and overall activity, for instance), the MOX and uranium cases are not much different. It is noteworthy, however, that the calculations show the 1-m dose rate for the MOX assembly to be about 150 rem/h at 100 years following discharge. This value is in excess of the canonical value of 100 rem/h.

Inspection of the dose-rate results for the uranium-fueled assembly shows that the values seem to scale with burnup. More appropriately, one needs to know the uncertainty on these calculations. Probably enough information is available on the uncertainty in cross-section estimates, for instance, such that an overall uncertainty could be calculated for the estimates we have made here. It is unlikely that such uncertainty analyses have been performed in a general sense for these types of estimates. The term "uncertainty analysis" does not mean a simple sensitivity analysis but rather an effort to estimate the uncertainty of all quantities used in the calculations and, in turn, to determine how these uncertainties propagate through the entire simulation.

As regards the actual nuclide inventories, the weapons-grade plutonium is definitely non-weapons grade at discharge. However, the results in Tables 4 and 5 show some noticeable differences between the two cases. It is possible that nuclides of interest in severe accident cases or from a criticality safety standpoint may cause different results in the MOX case as compared with the uranium case. However, one must keep in mind the following facts in assessing whether or not the differences between the two cases are significant in Tables 4 and 5. In the first place, one expects large differences for actinides because of the differences in fuel composition. Furthermore, because of the differences in total burn, one expects a MOX to LEU ratio of 0.88 if all else were equal. This trend can be seen for some of these nuclides. Finally, in the case of fission products with low yields, these yields may not be well known and therefore there may be differences between the two cases because these low-yield fission products result from different fissioning nuclides. Yields for some of these fissioning nuclides may actually be very different or, perhaps, it is simply the case that the low fission yield values are subject to varying degrees of uncertainty. One notes, however, that there is a significant difference in the ^{155}Gd predictions shown in Table 5. This is likely the result of differences in the ^{154}Gd capture cross sections because of neutron flux spectrum changes. Such a difference is to be expected although its magnitude in this case is surprising.

6. REFERENCES

1. *DOE Plutonium Disposition Study: Screening Study for Evaluation of the Potential for System 80+ to Consume Excess Plutonium*, Combustion Engineering, Inc., Windsor, Connecticut, April 30, 1994.

2. *SCALE: A Modular Code System for Performing Standardized Computer Analyses for Licensing Evaluation*, Vols. I–III, NUREG/CR-0200, Rev. 4 (ORNL/NUREG/CSD-2/R4), April 1995. Available from Radiation Shielding Information Center as CCC-545.

3. O. W. Hermann and R. M. Westfall, "ORIGEN-S: SCALE System Module to Calculate Fuel Depletion, Actinide Transmutation, Fission Product Buildup and Decay, and Associated Radiation Source Terms," Sect. F7 of *SCALE: A Modular Code System for Performing Standardized Computer Analyses for Licensing Evaluation*, Vols. I–III, NUREG/CR-0200, Rev. 4 (ORNL/NUREG/CSD-2/R4), April 1995. Available from Radiation Shielding Information Center as CCC-545.

4. J. R. Knight, C. V. Parks, S. M. Bowman, L. M. Petrie, and J. A. Bucholz, "SAS1: A One-Dimensional Shielding Analysis Module," Sect. S1 of *SCALE: A Modular Code System for Performing Standardized Computer Analyses for Licensing Evaluation*, Vols. I–III, NUREG/CR-0200, Rev. 4 (ORNL/NUREG/CSD-2/R4), April 1995. Available from Radiation Shielding Information Center as CCC-545.

5. O. W. Hermann and C. V. Parks, "SAS2H: A Coupled One-Dimensional Depletion and Shielding Analysis Code," Sect. S2 of *SCALE: A Modular Code System for Performing Standardized Computer Analyses for Licensing Evaluation*, Vols. I–III, NUREG/CR-0200, Rev. 4 (ORNL/NUREG/CSD-2/R4), April 1995. Available from Radiation Shielding Information Center as CCC-545.

6. O. W. Hermann, C. V. Parks, and J. P. Renier, *Technical Support for a Proposed Decay Heat Guide Using SAS2H/ORIGEN-S Data*, NUREG/CR-5625, ORNL-6698, U.S. Nuclear Regulatory Commission, September 1994.

7. M. A. McKinnon, T. E. Michener, M. F. Jensen and G. R. Rodman, *Testing and Analyses of the TN-24P PWR Spent-Fuel Dry Storage Cask Loaded with Consolidated Fuel*, EPRI NP-6191, Project 2813-16, PNL-6631, Interim Report, February 1989.

APPENDIX A

The SCALE System and Input Data to the Simulations

The SCALE system codes used in the simulations have been discussed in Sect. 4.1. Some files associated with these simulations are contained on a disk that is included as part of this report.

To summarize briefly, the SAS2H code sequence was used to simulate the burnup of the fuel assemblies studied. ORIGEN-S then made use of the output from SAS2H to calculate the isotopic composition and a number of other related quantities for the assemblies. ORIGEN-S also provided source terms that were used with the SAS1 code sequence to determine neutron and gamma fluxes and dose rates resulting from the spent fuel assemblies.

The files contained on the disk attached to this report are as follows:

MOXSAS2.IN: The input to SAS2H for the MOX (plutonium) case.

LEUSAS2.IN: The input to SAS2H for the low-enriched uranium (LEU) case.

MOXORG1.OUT: The ORIGEN-S output for the MOX fuel assembly at decay times of 1day, 3 days, 10 days, 30 days, 100 days, 1 year, 5 years, and 10 years.

MOXORG1.71: The source-term file from ORIGEN-S for the above decay times and to be used by SAS1.

MOXORG2.OUT: The ORIGEN-S output for the MOX fuel assembly at decay times 15 years, 30 years, 100 years, 300 years, 1,000 years, 3,000 years, 10,000 years, 30,000 years, 100,000 years, and 250,000 years.

MOXORG2.71: The source-term file from ORIGEN-S for the above decay times and to be used by SAS1.

LEUORG1.OUT, LEUORG1,71, LEUORG2.OUT, and LEUORG2.71 are the corresponding files for the LEU case.

MOXSAS1.IN: The input file to SAS1 for one unshielded MOX assembly.

LEUSAS1.IN: The input file to SAS1 for one unshielded LEU assembly.

MOXCSAS1.IN: The input file to SAS1 for 11 MOX fuel assemblies contained in a Transnuclear cask.

LEUCSAS1.IN: The input file to SAS1 for 11 LEU fuel assemblies contained in a Transnuclear cask.

INTERNAL DISTRIBUTION

1. C. W. Alexander
2. B. B. Bevard
3. S. M. Bowman
4. B. L. Broadhead
5. J. A. Bucholz
6. B. S. Cowell
7. M. D. DeHart
8. M. B. Emmett
9. N. M. Greene
10. S. R. Greene
11. O. W. Hermann
12. M. A. Kuliasha
13. L. C. Leal
14. S. K. Martin
15. G. E. Michaels
16. D. L. Moses
17-22. B. D. Murphy
23-28. L. F. Norris
29. J. V. Pace
30-34. C. V. Parks
35. L. M. Petrie
36-40. R. T. Primm, III
41. R. W. Roussin
42-46. J. C. Ryman
47. C. H. Shappert
48. D. J. Spellman
49. R. M. Westfall
50. B. A. Worley
51. R. Q. Wright
52-53. Laboratory Records Dept.
54. Laboratory Records, ORNL-RC Document Reference Section
55. ORNL Y-12 Research Library
56. Central Research Library
57. ORNL Patent Section

EXTERNAL DISTRIBUTION

58-63. M. Adams, Texas A&M University, Department of Nuclear Engineering, Zachry 129, College Station, TX 77843
64. J. Buksa, Los Alamos National Laboratory, P.O. Box 1663, Los Alamos, NM 87545
65. H. Canter, Department of Energy, Technical Director, 1000 Independence Ave., SW, Forrestal Building 3F043, Washington, DC 20585
66. T. Cremers, Los Alamos National Laboratory, P.O. Box 1663, Los Alamos, NM 87545
67. A. I. Cyeleman, Department of Energy, 1000 Independence Ave., SW, Forrestal Building 3F043, Washington, DC 20585
68. L. Groves, Sandia National Laboratories, P.O. Box 969, Livermore, CA 94551
69. D. Harrison, Department of Energy, 101 Convention Center Drive, Suite P200, Las Vegas, NV 89109
70. G. Holman, Lawrence Livermore National Laboratory, P.O. Box 808, Livermore, CA 94551
71. C. Jaeger, Sandia National Laboratories, P.O. Box 5800, Albuquerque, NM 87185-0759
72. Office of Scientific and Technical Information, Department of Energy, P.O. Box 62, Oak Ridge, TN 37831
73. Office of the ORNL Site Manager, Department of Energy, Oak Ridge National Laboratory, P.O. Box 2008, Oak Ridge, TN 37831
74. D. Peko, Department of Energy, 1000 Independence Ave., SW, Forrestal Building 3F042, Washington, DC 20585
75. P. T. Rhoads, Department of Energy, 1000 Independence Ave., SW, Forrestal Building 3F043, Washington, DC 20585
76. G. P. Rudy, Department of Energy, 1000 Independence Ave., SW, Forrestal Building 7B192, Washington, DC 20585
77. S. S. Sareen, Sandia National Laboratories, 2650 Park Tower Drive, Suite 800, Vienna, VA 22180

78. R. Zurn, Sandia National Laboratories, P.O. Box 969, Livermore, CA 94551